Fabrication of SiC-Type Films Using Low-Energy Plasma Enhanced Chemical Vapor Deposition (PECVD) and Subsequent Pyrolysis

Bryan Nguyen, Farnaz Tabarkhoon, Nicholas A. Welchert, Sheng Hu, Malancha Gupta, and Theodore Tsotsis *

Mork Family Department of Chemical Engineering and Materials Science, University of Southern California, 925 Bloom Walk, Los Angeles, California 90089, United States

*Corresponding Author Email: tsotsis@usc.edu

Abstract

Silicon carbide (SiC) is a promising material for a variety of applications in the biomedical, aerospace, and energy industries. Solution-phase techniques have long been used to deposit precursor films prior to pyrolysis into SiC, but they tend to face difficulties with substrate compatibility and the use of toxic solvents. In this study, we introduce a solventless synthesis route for fabricating SiC-type films by depositing an organosilicon copolymer poly(vinylphenyldimethylsilane-co-divinylbenzene) (p(VPDMS-co-DVB)) film using low-energy plasma chemical vapor deposition (PECVD) followed by subsequent pyrolysis. The chemical structure of the film was systematically studied in-situ during pyrolysis as a function of temperature using Diffuse Reflection Infrared Fourier Transform Spectroscopy (DRIFTS). The majority of the functional groups were found to have disappeared by a temperature of 800 °C, with most of the mass loss occurring between 350 °C and 520 °C. Thermogravimetric Analysis (TGA) was used to measure the loss of mass as the pyrolysis temperature was increased, and the observed pyrolysis rates were compared to estimates of such rates from the DRIFTS analysis. Our proposed synthesis route provides a scalable and solventless method of producing SiC-type ceramic films for such applications as high-temperature sensors and membranes.

Keywords: Silicon Carbide, Chemical Vapor Deposition, Pyrolysis

Introduction

Silicon carbide (SiC) has been shown to be a valuable material due to its high thermal conductivity, chemical resistance in corrosive (including acidic) environments, high mechanical stability, and low thermal expansion coefficient.[1,2] In addition, SiC has excellent dielectric properties and biocompatibility. Because of its versatility, SiC films have recently been finding many uses including, among others, a variety of biomedical[3] and electronic[4] applications. For example, in the aerospace field, SiC has been used in the manufacturing of nanoelectronic devices and integrated circuits as well as in the preparation of high-temperature sensors and actuators.[1] In addition to these applications, SiC/metal composites have been synthesized as a replacement for pure metals in order to reduce weight while retaining durable strength properties.[5] SiC membranes have also been used as both macroporous and microporous filters, for applications such as wastewater treatment[6] and hydrogen gas separations[7].

SiC thin films can be fabricated using solution-phase[8] and gas-phase[9] techniques, both of which have been studied by our group. Processes such as dip-coating[10] and polymer infiltration have been popular methods for depositing precursor SiC films on underlying supports prior to pyrolysis[11]. Solution-phase techniques, however, usually have substrate compatibility issues, and also pose safety and environmental concerns due to the use of toxic solvents.[12] As a result, in addition to the solution-phase processes, a variety of chemical vapor deposition (CVD) techniques, including hot-wall chemical vapor deposition (HWCVD)[13, 14] and plasma-enhanced chemical vapor deposition (PECVD),[15, 16, 17] have also been used to prepare SiC films with sub-micron thicknesses using organosilicon precursors or a combination of silane and gaseous hydrocarbons as a source.

Previously, Pagès et al. deposited, via high-energy PECVD, SiC membrane films on porous alumina tubes using diethylsilane as a precursor, Ar as the ionizing gas, and employing a substrate temperature of 300 °C.[18] Huran et. al deposited SiC films on silicon wafers via PECVD using SiH_4 and CH_4 with flow rates of 10 sccm and 40 sccm, respectively, and a deposition temperature of 450 °C.[19] Similarly, Wei et al. deposited amorphous SiC films on silicon wafers using SiH_4, CH_4, and Ar with flow rates of 70, 500, and 700 sccm, respectively, a deposition temperature of 400 °C, and plasma power of 600 Watts.[20] Despite its success in preparing SiC films, high-energy PECVD

has a number of shortcomings. Because it requires high energy inputs and substrate temperatures, the technique is not appropriate for applications requiring temperature-sensitive substrates like those, for example, employing sacrificial porous polymer templates such as polyurethanes with low degradation temperatures.[21] The aim to directly, in one step, produce SiC, in addition to dictating the use of high temperatures and power densities, also limits the availability of appropriate gaseous precursors to mostly silanes with or without low molecular weight hydrocarbon (e.g., CH_4) co-reactants. In addition, the ceramic yield of these reactors is, typically, quite low, thus dictating the use of high precursor flow rates. For the production of nanoporous SiC membrane and sensor films deposited on underlying macroporous supports, which is the focus of our own research, it is difficult to use the high-energy PECVD technique and still be able to prevent infiltration of the precursors which leads to SiC formation deep into the structure of the underlying support, which then adversely impacts the permeability of the resulting membrane materials.

In this paper we propose, instead, the use of low-energy PECVD to fabricate SiC films on underlying supports. In contrast to directly forming the SiC film on the support, like in the case of high-energy PECVD, our technique, similarly to solution-phase methods, first prepares a precursor pre-ceramic polymer film, and then converts it, in a subsequent step, via pyrolysis into a SiC film. However, our technique avoids the common shortcomings of the solution-phase methods noted above.

We applied previously a similar two-step approach to prepare silica microporous membrane films[22], during which we deposited a cross-linked siloxane polymer film on macroporous supports using, however, a different technique called initiated chemical vapor deposition (iCVD). We subsequently pyrolyzed these pre-ceramic films to form membranes capable of separating helium from its binary mixtures with larger molecules (e.g., argon) through a molecular sieving mechanism. Unlike PECVD, iCVD uses an initiator, typically, a peroxide compound, to initiate free-radical polymerization of monomers.[23] For the fabrication of SiC precursor polymer films, it is important to limit the amount of oxygen embedded in the backbone of the polymer to avoid it from being incorporated into the structure of the resulting ceramic film, which makes it challenging to prepare such films using iCVD. It is possible to convert siloxane

moieties directly into SiC, but it typically requires the use of much higher temperatures or employing an additional carbon source.[24] Low-energy PECVD, in contrast to iCVD, does not require the use of an initiator molecule. In low-energy PECVD, a low-energy plasma is used to initiate the reactions between chemical species to prepare a variety of organic films while employing low precursor flow rates and relatively low substrate temperatures (<100 °C).[25, 26, 27] The technique has been used to deposit homogeneous films on large area substrates, and such films tend to be more cross-linked and to have stable chemical and physical features.[28] Increased cross-linking in the structure of the precursor polymer has been shown to help improve the ceramic yield during film pyrolysis.[2] The technique is amenable to "roll-to-roll" processing,[29] to produce large-area, uniform precursor polymer films that can then pyrolyzed to produce large-area inorganic SiC-type films with correspondingly large areas.

In this project, we study the deposition of the pre-ceramic polymer films on porous substrates using low-energy PECVD, and subsequently pyrolyze these films to produce SiC-type ceramic films. We systematically study the deposition of the polymer at various monomer flow rate ratios. We also analyze the structural changes of the polymer as it undergoes pyrolysis to eventually form a SiC-type ceramic and examine the kinetics of the pyrolysis process. To our knowledge, we are the first group to study the pyrolysis of PECVD-deposited polymer films to form inorganic SiC-type films.

Experimental

PECVD Deposition

A schematic of the lab-scale low-energy PECVD reactor used in this study to deposit the various polymer films is shown in Figure 1. It is a cylindrical reactor chamber, 250 mm in diameter and 48 mm in height, purchased from the GVD Corporation. The reactor operates under vacuum conditions via the use of a rotary-vane vacuum pump (Edwards E2M40). For the experiments in this paper, the reactor pressure was maintained at 180 mTorr using a feedback-type, throttle-valve controller (MKS 153D) with the aid of a capacitance manometer (MKS 622C01TDE Baratron). The temperature of the deposition stage inside reactor was kept constant at 50 °C using a recirculating bath chiller (Thermo Scientific NESLAB RTE 7).

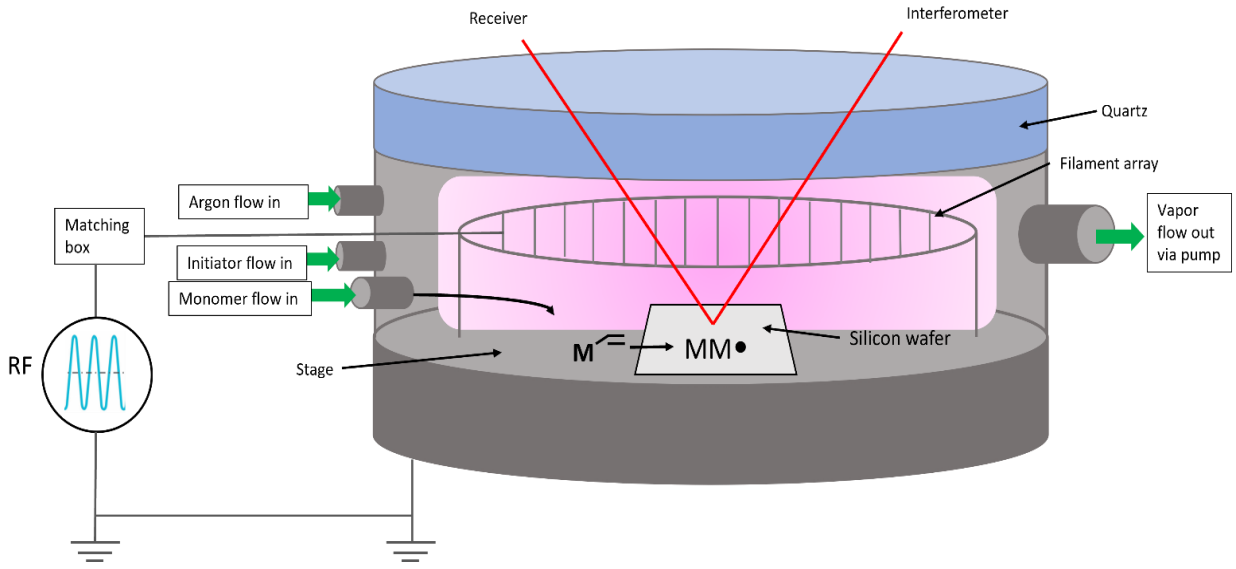

Figure 1: Schematic of the PECVD reactor.

Prior to initiating film deposition, we identified a number of organosilicon candidate monomers, all of which had physical properties amenable to low-energy PECVD deposition and chemical structures pre-disposed to form SiC-type films upon pyrolysis; they varied in the type of organic moieties they contained. Among these candidate monomers, we selected for further study vinylphenylmethylsilane (VPDMS) because it forms polymers with phenyl pendant groups which tend to have good SiC yields post-pyrolysis.[2] We also selected divinylbenzene (DVB) as a cross-linker, since it has been shown that cross-linked pre-ceramic polymers tend to have higher ceramic yields.[2] Figure 2 shows the chemical structures of VPDMS and DVB.

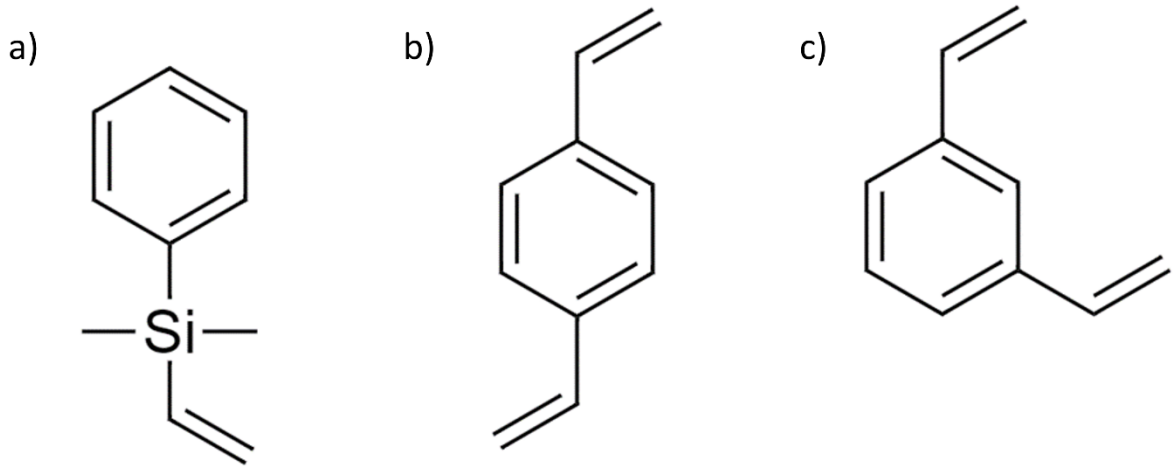

Figure 2: The chemical structure of the a) VPDMS, b) para-DVB and c) meta-DVB monomers.

The VPDMS (Gelest, 95%) and DVB (Aldrich, 80%) monomers were used as received without further purification. They were loaded into stainless steel jars that were then mounted onto the reactor; the temperature of both jars was kept constant at 25 °C. The monomers were introduced into the reactor via heated lines maintained at a temperature of 40 °C. The VPDMS and DVB flow rates were varied between 1.8 and 4.0 sccm, depending on the desired molar flow ratios. Argon gas (99.999% pure) was also fed into the reactor as the ionizing gas, and its flow rate was maintained at 40 sccm using a mass flow controller (MKS Type 1479A). Prior to the deposition, the chamber of the reactor was purged six times in order to reduce the oxygen content of the ambient environment. This was done by slowly increasing the reactor pressure from vacuum to a positive pressure using argon gas. In addition, all of the lines were held under vacuum prior to the deposition in order to further reduce the oxygen content. We studied the deposition of the pre-ceramic polymer film onto two different powder substrates, potassium bromide (KBr, Alfa Aesar) and barium fluoride (BaF_2, Aldrich, 99.95%). The deposition rate on the powder substrates was determined by measuring in situ via interferometry with a He-Ne laser (Industrial Fiber Optics, 633 nm) the deposition rate on a reference silicon wafer (Wafer World 119) placed nearby on the reactor stage.

We used an external radio frequency (RF) plasma generator (Diener; 13.56 MHz, 100 W) with a manual matchbox (Diener) which was connected to a nichrome filament array (Omega Engineering, 80%/20% Ni/Cr) positioned 4.6 cm above the reactor stage. The nichrome filament

served as the electrode to spark and generate the plasma. The RF plasma generator was operated at 35 W.

Chemical Characterization

To analyze the chemical structure of the polymer films, we measured their IR absorbance spectra ex situ using a FTIR spectrophotometer (Nicolet iS10, Thermo Scientific). For such measurements, the films (~1 μm thick, as measured via interferometry) were deposited onto clean silicon (Si) wafers. The clean bare Si wafer was also used as the background for the spectra. To acquire the monomer IR spectra, a drop of liquid monomer was sandwiched in between two Si wafers and the IR spectrum taken, with two Si wafers being used as the background.

To analyze the change in the polymer structure as a function of temperature during pyrolysis, we used Diffuse Reflectance Infrared Fourier Transform Spectroscopy (DRIFTS, COLLECTOR II, Thermo Scientific). The DRIFTS technique allows for monitoring the change in the IR spectra of a powder substrate in situ as the sample is heated to the desired temperature.[40] To prepare the polymer-coated powder samples for the DRIFTS experiment, the KBr and BaF_2 powders were spread manually with the aid of a razor blade onto a Si wafer. The polymer was then deposited onto the powder-covered wafers. The film deposition was allowed to proceed until a nearby bare Si substrate was coated with a ~ 2 μm thick polymer film. The polymer-coated powders were then inserted into the DRIFTS sample cup and leveled with a razor blade, as instructed in the instrument manual.[30] The DRIFTS apparatus was then closed and heated at a temperature of 100 °C, under flowing ultra-high purity (UHP) Ar at a pressure of 170 kPa for 2 hr in order to eliminate any moisture effects and to ensure an inert atmosphere during pyrolysis. For the DRIFTS measurements, the cell was heated at a rate of 1 °C/min from a temperature of 100 °C to 800 °C, which is the maximum operating temperature of the high temperature and pressure DRIFTS cell used in this experiment. The IR absorbance spectra were recorded at 20 °C temperature intervals, or approximately every 20 min. After every temperature rise interval of 100 °C, the increase in temperature was stopped and the samples were allowed to stay ("soak") at that temperature for 1 hr. During this pyrolysis period under isothermal conditions, the IR absorbance spectra were again recorded every 10 min. Uncoated KBr and BaF_2 powders were used as the background spectra for the polymer-coated KBr and BaF_2 powders.

The polymer-coated BaF_2 powder was also pyrolyzed up to a higher temperature (1000 °C) outside the DRIFTS cell. For that, the powder was placed inside a graphite furnace, evacuated first, and then purged with UHP Ar for 1 hr to eliminate potential oxygen contamination. After six cycles of evacuation and purging, the powder was heated at a rate of 1 °C/min in flowing Ar up to a temperature of 1000 °C. As with the DRIFTS experiments, for every 100 ºC interval, the ramping of temperature was stopped, and the sample was kept at that temperature for 1 hr. After the temperature reached 1000 °C, the powder was kept at that temperature for 3 hr, after which it was cooled back to room temperature at a rate of 3 °C/min. The slow heating and cooling rates were chosen because they have been shown previously to prevent cracking during the preparation of ceramic materials.[31] After being cooled down to room temperature, the powder was placed in the DRIFTS sample cup, and the chamber was purged with Ar for 30 min before IR absorbance spectra were taken. The DRIFTS and FTIR spectra were both analyzed using the freeware SpectraGryph 1.2. and the deconvolution was performed using OriginPro Peak Analyzer.

For the atomic composition and surface analysis of the polymers, a plasma focused ion beam (PFIB)/scanning electron microscope (SEM) system was utilized (Thermo Scientific, Helios G4 PFIB UXe DualBeam FIB/SEM). The microscope is equipped with an x-ray energy dispersive spectroscopy (EDS) system for elemental analysis equipped with an Oxford UltimMax 170 Silicon Drift Detector. Data were collected with a voltage of 10 kV and a 1.6 nA beam current. The working distance of the apparatus was set to 5.6 mm and for each spectrum, 1,000,000 counts was chosen as the setting.

Thermogravimetric Analysis

Thermogravimetric analysis (TGA, Cahn Instruments, 12130-01) was used to measure the mass loss of the polymer during pyrolysis as a function of temperature. For the analysis, approximately 100 mg of the polymer-coated BaF_2 powder was placed inside the cup of the TGA apparatus. The TGA chamber was then purged with flowing Ar (flow rate of 30 sccm) for 20 min. The powder was heated (ramp rate of 3 °C/min) to 100 °C and allowed to rest there for 2 hr under flowing Ar in order to eliminate any residual sample moisture. Then, the sample was heated from 100 °C to 300 °C at a ramp rate of 2 °C/min, and subsequently in increments of 100 °C from 300 °C to 900 °C at a ramp rate of 5 °C/min, with soaking times of 1 hr at the end-point of each 100 °C heating interval.

Film Thickness Measurement

The change in the thickness of the films deposited on bare silicon wafers before and after polymer pyrolysis was measured using a stylus profilometer (AMBiOS XP-2). The scan length was set at 5 mm.

Results and Discussion

Polymer Film Analysis Using FTIR

PECVD was used to deposit five different polymer films: poly(vinylphenyldimethylsilane) (pVPDMS), poly(divinylbenzene) (pDVB), and three poly(vinylphenyldimethylsilane-co-divinylbenzene) (p(VPDMS-co-DVB)) copolymers employing VPDMS:DVB feed flow rate ratios of 1:1, 2:1, and 1:2. Figure 3 shows the transmission FTIR spectra of the pVPDMS, the pDVB, and the p(VPDMS-co-DVB) copolymers prepared by the PECVD technique on Si wafers as well as of the monomers themselves (for a reference to the various IR bands in this and subsequent Figures, please see Table 1). The monomers contain vinyl stretching bands (region iia and iib) at approximately 903 cm^{-1} and 990 cm^{-1}. For the pVPDMS and pDVB polymers as well as the copolymers, the vinyl bands are significantly reduced, something which has also been reported previously by other investigators.[32] The reduction of the vinyl stretching bands area (region iia and iib) is accompanied by an increase in the ethylene backbone C-H stretching bands (region viia) at approximately 2940 cm^{-1} formed during the polymerization reaction.

Table 1. IR bands shown in Figures 3-8

Regions	**IR Bands Corresponding to Bonds**
ia	meta-substituted benzene vibrations
ib	para-substituted benzene vibrations and Si-C stretching
iia	δ(=C-H) modes of the vinyl bond in DVB
iib	wagging in CH_2 of vinyl bond in VPDMS
iiD	CH_2 deformations in Si-$(CH_2)_n$-Si
iii	Si-C_6H_5 stretching
iv	symmetric Si-CH_3 stretching

v	aromatic C-C/C=C ring stretches for m-DVB and p-DVB
vi	Si-H stretching
viia	C-H hydrocarbon bonds from polyethylene bonds and pendant vinyl bands
viib	C-H stretching from hydrocarbon bonds in aromatic rings

The increase in these bands is particularly noticeable in the pDVB and the 1:1 and 1:2 VPDMS:DVB copolymer films, indicating that the increased incorporation of the methylene bridges result from the DVB polymerization.[33] The decrease of the DVB monomer bands between 700 and 850 cm^{-1} (region ia and ib) are indicative of decrease of the meta and para vibrations of the benzene ring, as has previously been seen by iCVD polymerization of DVB.[33] The bands between 3000 and 3100 cm^{-1} (region viib) are attributed to the various v(=C-H) modes of the aromatic rings. Their continued presence in the spectra, as the polymer is being deposited, is indicative of the fact that the polymerization reaction occurs primarily through the vinyl bonds. The methyl ($Si-CH_3$) stretching bands at 1250 cm^{-1} (region iv) which are prominent in the VPDMS spectra also remain in the pVPDMS polymer and in the p(VPDMS-co-DVB) copolymer spectra, indicating that these bonds have remained relatively intact during polymerization.[34] The aromatic (C_6H_5) C-C and C=C (region v) stretching bands between 1300 and 1600 cm^{-1} that are prominent in both the VPDMS and DVB spectra are still present in the pVPDMS and in the p(VPDMS-co-DVB) copolymer spectra, again indicating that these bonds remained relatively intact during polymerization.[13] In addition, the Si-C stretching band (region ib) between 700 and 900 cm^{-1} also remains intact in both the pVPDMS and the p(VPDMS-co-DVB) copolymers. This peak size is noticeable in the pVPDMS, 1:1, and in the 2:1 VPDMS:DVB copolymer film spectra, but is reduced in the 1:2 VPDMS:DVB spectra, indicating that there is much less VPDMS incorporated in the polymer prepared using this volumetric flow rate ratio. There is also a small band around 2100 cm^{-1} (region vi) corresponding to the Si-H stretching vibration in all of the deposited polymers films (except pDVB), which is, potentially, indicative of a small degree of polymer (Si-C bond) cleaving.[35]

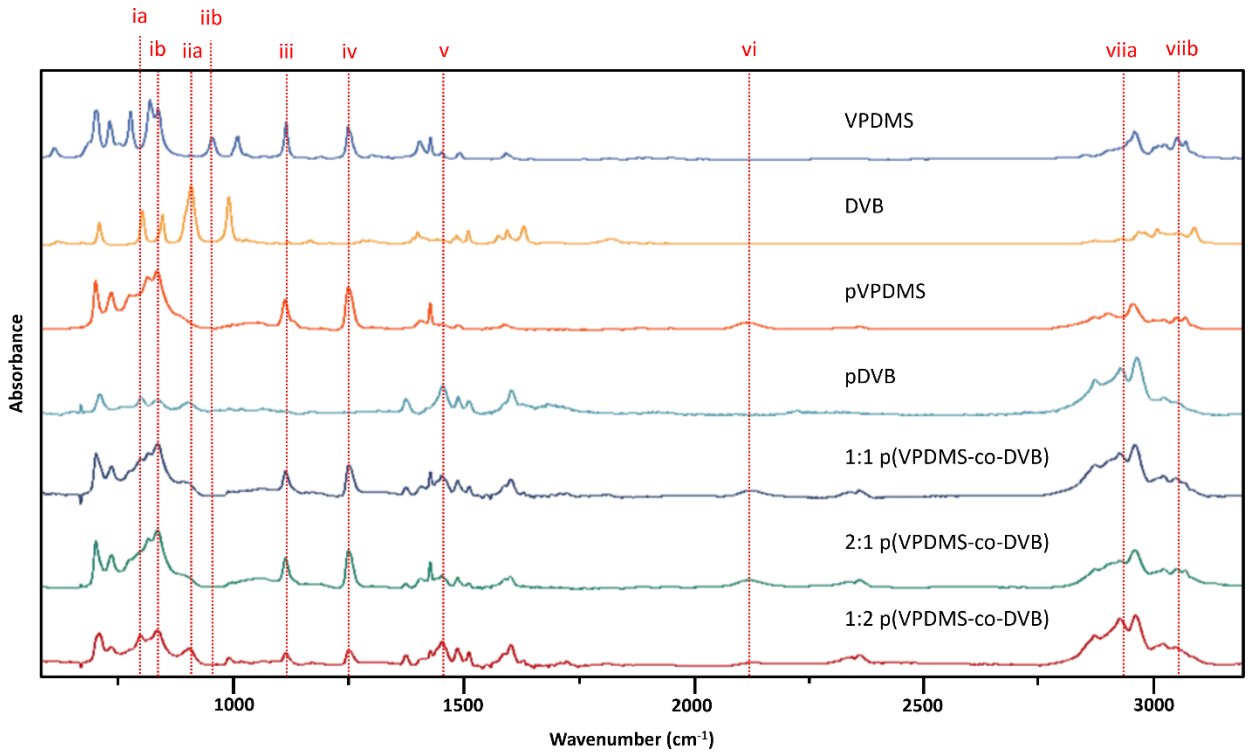

Figure 3. FTIR spectra of PECVD-deposited polymer films deposited on Si wafers. The dashed lines represent regions: (i) Si-C stretching and para- and meta-vibrations of DVB ring, (ii) vinyl bond stretching, (iii) Si-C_6H_5 stretching, (iv) symmetric Si-CH_3 stretching, (v) aromatic C_6H_5 C-H and C=C stretching bands, (vi) Si-H stretching, and (vii) C=C and C-H hydrocarbon bonds from polyethylene bonds and aromatic rings.

In both the pDVB and the copolymer spectra, the majority of the vinyl bands are reduced, indicating that most of the vinyl bonds have reacted and the polymer is, therefore, thoroughly cross-linked. To confirm that the copolymer was, indeed, cross-linked, we investigated the solubility of such films deposited on Si wafers in acetone at room temperature. After performing a number of solubility tests, we found that the pDVB film was insoluble in acetone, while the pVPDMS film completely dissolved in it. The copolymer films, similarly to the pDVB film, were also not soluble in acetone, which indicates that they are, likely, also cross-linked.

The atomic carbon to silicon (C/Si) ratio in the precursor film plays an important role in determining the composition of the final ceramic film, in particular its carbon content. To measure this ratio, we carried out EDS measurements in order to determine the atomic composition of the films. EDS has been shown previously to be an effective method for determining the elemental

composition of silicon-based polymer films.[36,37] Table 2 shows the atomic composition of each film based on the EDS testing.

Table 2. Atomic Composition of the Deposited Polymer Films from EDS Analysis

Sample	Spot	Atomic Composition				C:Si Ratio	Theoretical C:Si Ratio	Si:O Ratio
		C	Si	O	Other			
pVPDMS	1	89.2	8.9	1.7	0.1	10.0	10	5.2
	2	89.1	8.9	1.8	0.1	10.0		4.9
	3	89.2	8.9	1.8	0.2	10.0		4.9
pDVB	1	93.1	0.1	6.8	0	-	-	-
	2	93	0.1	6.9	0	-		-
	3	93	0.1	6.9	0	-		-
1:1	1	94.7	3.8	1.4	0.1	24.9	20	2.7
	2	94.7	3.8	1.4	0.1	24.9		2.7
	3	94.8	3.8	1.4	0.1	24.9		2.7
2:1	1	94	4.4	1.6	0	21.4	15	2.8
	2	94	4.4	1.6	0	21.4		2.8
	3	94	4.4	1.6	0	21.4		2.8
1:2	1	96.1	2.5	1.4	0	38.4	30	1.8
	2	96.1	2.5	1.4	0	38.4		1.8
	3	96	2.5	1.5	0	38.4		1.7

We analyzed three different spots on each sample, with at least a distance of 1 mm apart from each other; for each spot, we carried out three different measurements, with the average composition value for each spot shown in Table 2. As Table 2 indicates, the composition of the different spots is quite similar, which signifies spatially uniform deposition kinetics. All films were shown to be carbon rich, as expected from the original (C/Si) ratios of both the VPDMS and DVB monomers. Previous studies[38] have shown that increasing the plasma energy during PECVD, beyond 100 Watts, generally, resulted in decreased carbon content of the resulting polymer; this is, likely, due to the cleavage of various functional monomer moieties taking place during the polymerization process. Because we utilize relatively low power (<40 Watts) during our PECVD studies, the retention of carbon was very high, as can be seen from the (C/Si) ratio of the pVPDMS film that matches that of the original monomer. For the copolymer films, the (C/Si) ratio is higher

(24 -25%) than the predicted value based on the feed volumetric flow rate ratios (on the assumption that they incorporate into the structure of the growing polymer at rates which are proportional to their flow rates). This indicates that during the formation of these copolymers, the DVB monomer incorporates at a faster rate into the growing polymer chain than the VPDMS, thereby resulting in a greater carbon content in its structure.

In all polymer films, we find a small oxygen content (the silicon to oxygen (Si/O) ratio is also included in the Table). Since neither monomer contains oxygen, its presence in the EDS spectrum of the final polymer may signify either oxygen incorporation during the preparation of the films, as a result of trace oxygen contaminants being present in the PECVD chamber, or due to exposure to the laboratory air during the transfer step from the PECVD chamber to the SEM/EDS laboratory. It should be also noted that the DVB monomer contains an inhibitor (4-tert-butylpyrocatechol, 1-5 %) which has oxygen in its structure, so it is conceivable that this inhibitor may have been incorporated into the polymer structure during the deposition (this may also explain the lower Si/O ratio of the copolymer films relative to pVPDMS). There are no peaks at the Si-O-Si position of the FTIR spectra, so the oxygen in the polymer films is, likely, either adsorbed oxygen (or hydroxyls) as a result of exposure to laboratory air, or due to C=O bonds being formed during the polymer deposition process.

Study of the Pyrolysis Process Using DRIFTS

The transformation of the polymer film into a ceramic during pyrolysis was studied using the DRIFTS technique. For that, the polymer was deposited, via PECVD, onto two different powder substrates, made of KBr and BaF_2, in order to investigate whether the substrate itself influences the composition and/or structure of the ceramic produced. We have previously used the DRIFTS technique to study the scission of functional groups during the pyrolysis of a polymer film and its conversion into a ceramic.[8] Other groups[39,40,41] have also used the DRIFTS technique to study the heat treatment of organosilicon materials to produce siloxane films.

Figure 4 shows the DRIFTS data generated during the pyrolysis of the 1:1 VPDMS:DVB copolymer coated on KBr powder. The DRIFTS cell was heated at a rate of 1 °C/min from a temperature of 100 °C to 700 °C (the maximum operating temperature of our DRIFTS cell is 800 °C) since the melting temperature of KBr is ~734°C. The IR absorbance spectra were recorded at 20 °C temperature intervals, or approximately every 20 min. After every temperature rise interval

of 100 °C, the increase in temperature was stopped and the samples were allowed to "soak" at that temperature for 1 hr. During the "soak" pyrolysis period under isothermal conditions, the IR absorbance spectra were again recorded every 10 min. Comparing the spectra for the starting (not pyrolyzed) polymer coated onto the KBr powder in Figure 4 to the corresponding FTIR spectra of the same polymer coated on a Si wafer in Figure 3, it can be concluded that the major bands in both spectra are the same. They include the Si-C stretching band at ~800 cm^{-1} (band i in Figure 3), the phenyl stretching band at 1100 cm^{-1} (band iii), the methyl symmetric stretching band at 1260 cm^{-1} (band iv), the Si-H peak at approximately 2100 cm^{-1} (band vi), and the backbone C-H stretching bands between 2920 and 3000 cm^{-1} (band vii). The various benzene ring C-C and C=C stretching bands of pDVB are located between 1400 and 1600 cm^{-1} (band v).

From the spectra in Figure 4, it can be concluded that there are no significant changes that take place in the structure of the polymer until a pyrolysis temperature of ~300 °C is reached. Between a temperature of 300 °C and 400 °C, the Si-H stretching band (band vi, ~2100 cm^{-1}) decreases significantly. In addition, the methyl stretching band (band iv) and the Si-C_6H_5 stretching bands (band iii) both decrease. The various stretching bands associated with pDVB (band v) decrease as well, likely indicating that some of the rings have started to cleave or decompose. Straus et al.[42] who previously studied the pyrolysis of pDVB also found that at temperatures between 300 °C and 400 °C, the carbon bonds in the pDVB ethylene chain break to form monomers, dimers, and trimers.

By a pyrolysis temperature of 500 °C, the stretching bands for most of the organic groups have substantially decreased, and there is also a significant decrease in the ethylene band at 2920 cm^{-1} (band vii). The disappearance of these bands represents a similar behavior to that we have previously seen[14] during the pyrolysis of organosilicon polymers, where the majority of the functional groups cleave at pyrolysis temperatures greater than 400 °C. Schiavon et. al.[43], during pyrolysis experiments with cyclical polysiloxane composites using DRIFTS, also found that the majority of the C-H bands disappeared in this temperature range.

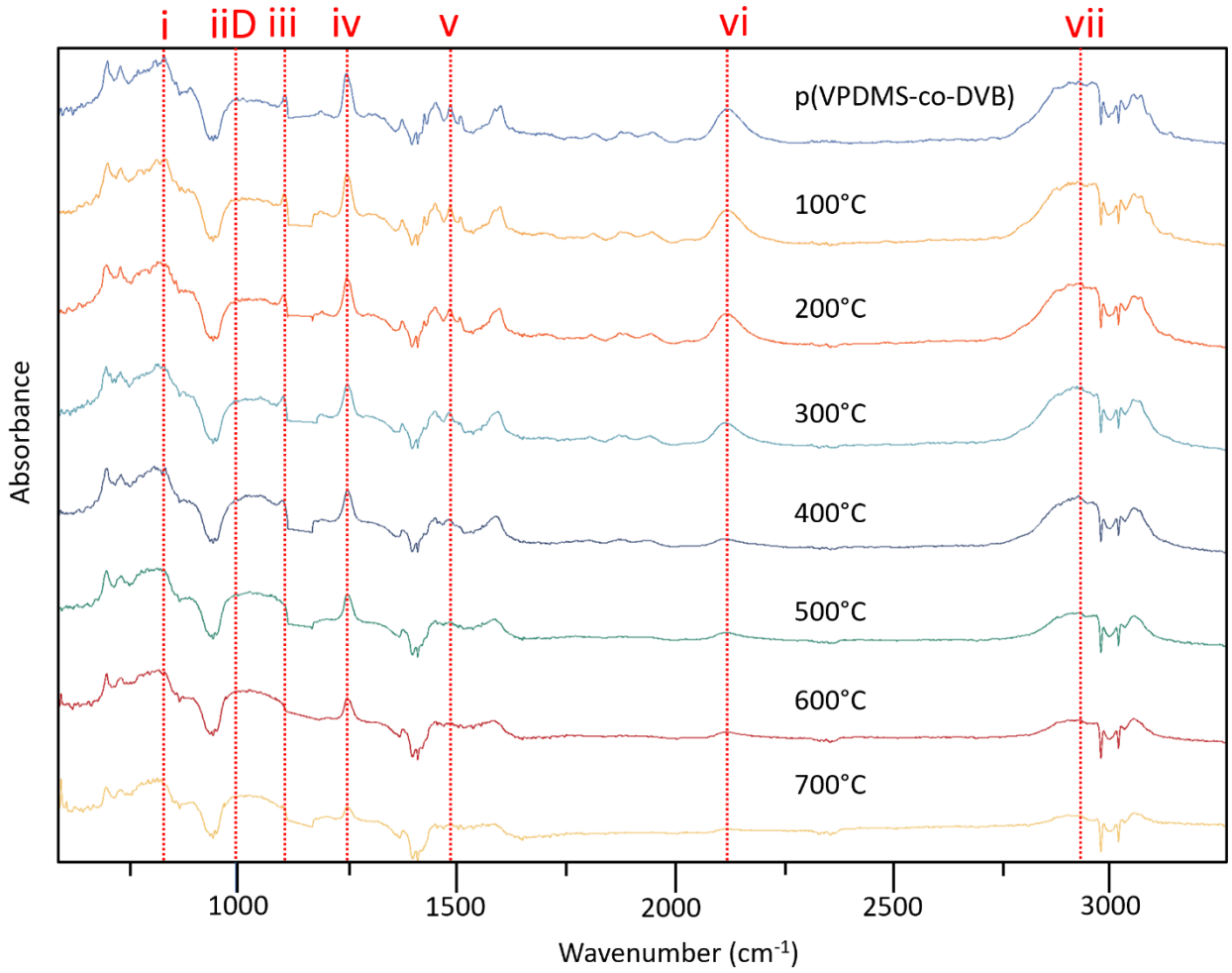

Figure 4: DRIFTS data during pyrolysis for the copolymer coated on KBr. The dashed lines represent: (i) Si-C stretching, (iiD) Si-$(CH_2)_n$-Si stretching, (iii) Si-C_5H_6 stretching, (iv) symmetric Si-CH_3 stretching, (v) pDVB C-H and C=C stretching bands, (vi) Si-H stretching, and (vii) C-H hydrocarbon bonds from polyethylene bonds and aromatic rings.

By a pyrolysis temperature of ~600 °C, most of the phenyl (band iii) and methyl stretching vibration (band iv) bands have completely disappeared, and the ethylene stretching band has largely vanished as well. Through this pyrolysis process, the Si-C stretching band around 800 cm^{-1} (band i) has remained prominent, likely, indicating that the silicon-carbon bond has stayed intact in the structure. The final structure that is observed after a pyrolysis temperature of 700 °C consists of a Si-C network with small amounts of Si-$(CH_2)_n$-Si (band iiD) being present as well. There are, however, residual organic functional groups remaining in the spectra, as indicated by the presence of methyl and polyethylene stretching bands.

We have also studied, via DRIFTS, the pyrolysis of copolymer films deposited on BaF_2 powder. Using BaF_2 instead of KBr is advantageous because its melting temperature is 1368 ºC, and, thus, it can withstand higher pyrolysis temperatures. Figures 5, 6, 7, and 8 show the results from the pyrolysis of BaF_2 powders coated with pVPDMS, 1:1 VPDMS:DVB, 2:1 VPDMS:DVB, and 1:2 VPDMS:DVB polymers. The range of pyrolysis temperatures in these Figures is broader than those in Figure 4, ranging up to 800 °C, the limit of the DRIFTS cell.

Similarly with the spectra of the polymer-coated KBr powder, the DRIFTS spectra of the polymer-coated BaF_2 powders show the same peaks as those in the FTIR spectra of the same polymers coated on Si wafers, shown in Figure 3. For all four polymers, there were no major changes in the spectra up to a pyrolysis temperature of ~300 °C. In the spectra taken at a temperature of 400 °C, we observe a reduction in the size of several bands, including the Si-H stretching band (band vi) at ~2100 cm^{-1} and the phenyl Si-C_6H_5 stretching band (band iii) at ~1100 cm^{-1}. In addition, there is a slight reduction in the methyl stretching band at 1260 cm^{-1} (band iv) and of the backbone C-H bands around 2980 cm^{-1} (band vi). Moreover, for the 1:1 and 1:2 VPDMS:DVB copolymers, the pDVB-related stretching band ~1350 cm^{-1} (band v) is significantly reduced, and there is also a slight increase in the band around 1000 cm^{-1} (band iiD), assigned to the Si-$(CH_2)_n$-Si stretching vibration. An increase of the band assigned to Si-$(CH_2)_n$-Si between 400 °C and 600 °C was also observed by Breuning[19] during the heat treatment of a polysilazane polymer, and it can be attributed to the rearrangement of bonds to form carbon bridges between silicon atoms. The higher incorporation of DVB monomer in the 1:1 and 1:2 VPDMS:DVB copolymers seems to have led to a larger increase in the formation of hydrocarbon bridges, while no such bridges are observed forming for the 2:1 VPDMS:DVB copolymer which has less DVB incorporated in its structure. We did not observe the formation of such bridges for the pVPDMS polymer, so it can be concluded that the presence of DVB has an important role in the formation of these hydrocarbon bridges.

In the spectra taken at a pyrolysis temperature of 600 °C, the backbone and the methyl stretching bands (bands vii and iv, respectively) have significantly decreased in size. The size of the aromatic stretching bands (band v) has decreased as well. For the 1:1 and 1:2 VPDMS:DVB copolymers, these bands are much more prominent than their counterparts in the pVPDMS and 2:1 VPDMS:DVB copolymer spectra. However, by a pyrolysis temperature of 700 °C, these bands have largely disappeared from the spectra of all polymers studied. In the spectra taken at the

temperature of 800 °C, the bands for Si-$(CH_2)_n$-Si (band iiD) substantially decrease for the 1:1 and 2:1 VPDMS:DVB copolymers, indicating the conversion of these groups into a Si-C network. However, for the 1:2 copolymer, the Si-$(CH_2)_n$-Si band is still quite prominent, again indicating the impact the increased presence of DVB in the copolymer precursor has on the composition of the resulting ceramic. The film from pyrolysis at 800 °C consists, largely, of a Si-C network structure with a few functional groups along with residual Si-$(CH_2)_n$-Si segments remaining in the network. These results agree with the KBr DRIFTS results, and they confirm that a Si-C$_X$-type of material is produced at elevated pyrolysis temperatures.

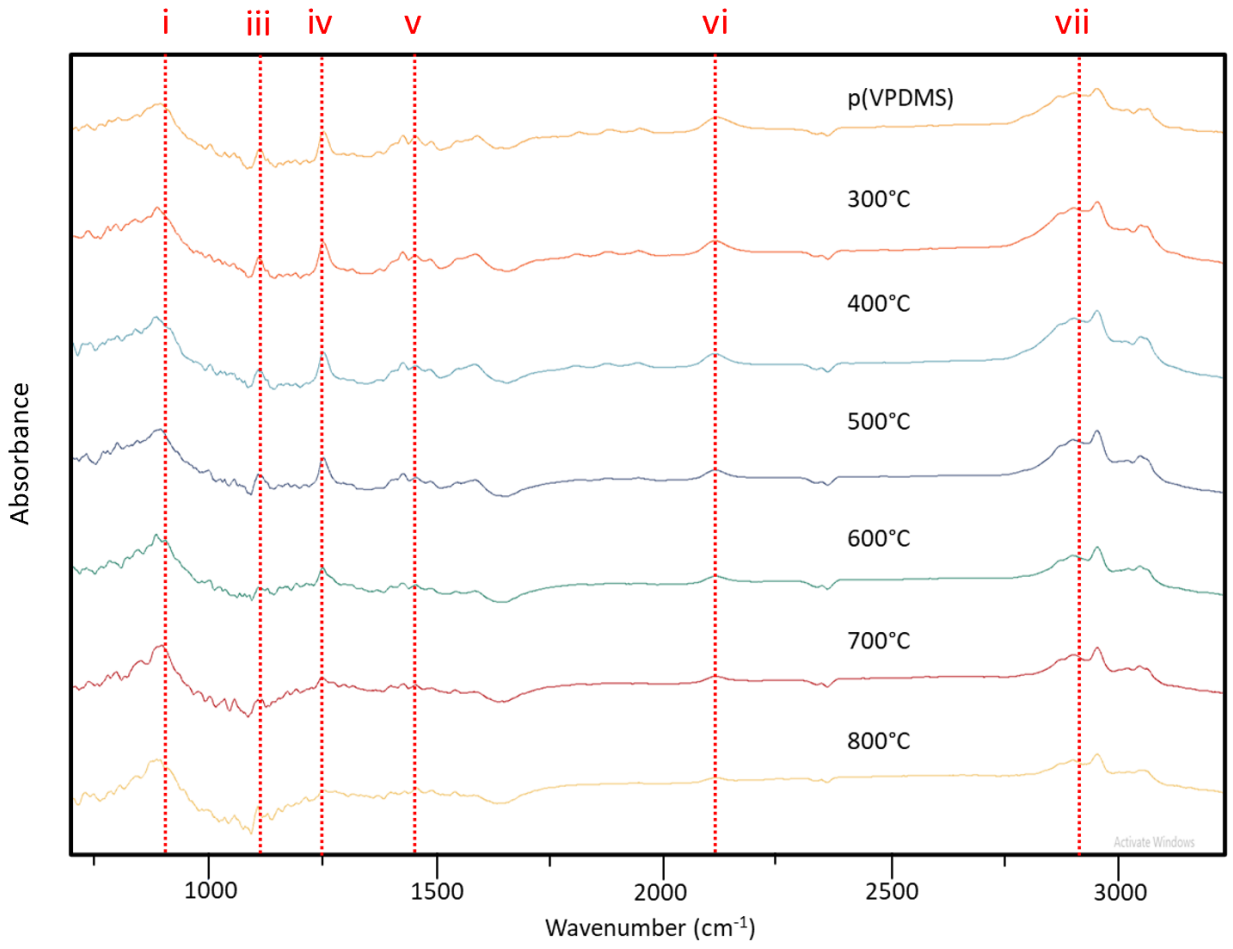

Figure 5: DRIFTS data for the pVPDMS-coated BaF_2. The dashed lines represent: (i) Si-C stretching, (iii) Si-C_5H_6 stretching, (iv) symmetric Si-CH_3 stretching, (v) pDVB C-H and C=C stretching bands, (vi) Si-H stretching, and (vii) C-H hydrocarbon bonds from polyethylene bond and aromatic rings.

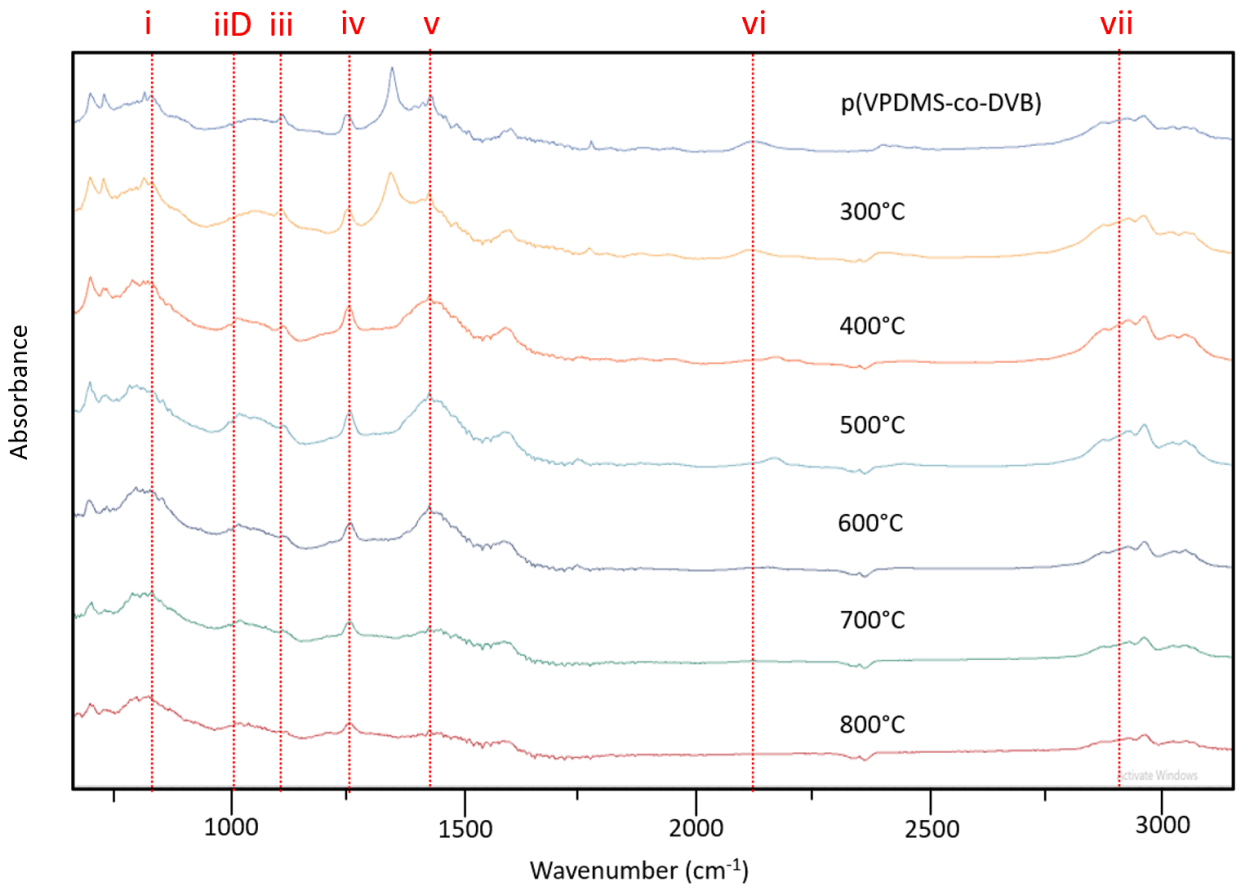

Figure 6: DRIFTS data for the 1:1 p(VPDMS-coDVB)-coated BaF_2. The dashed lines represent: (i) Si-C stretching, (iiD) Si-$(CH_2)_n$-Si stretching, (iii) Si-C_5H_6 stretching, (iv) symmetric Si-CH_3 stretching, (v) pDVB C-H and C=C stretching bands, (vi) Si-H stretching, and (vii) C-H hydrocarbon bonds from polyethylene bond and aromatic rings.

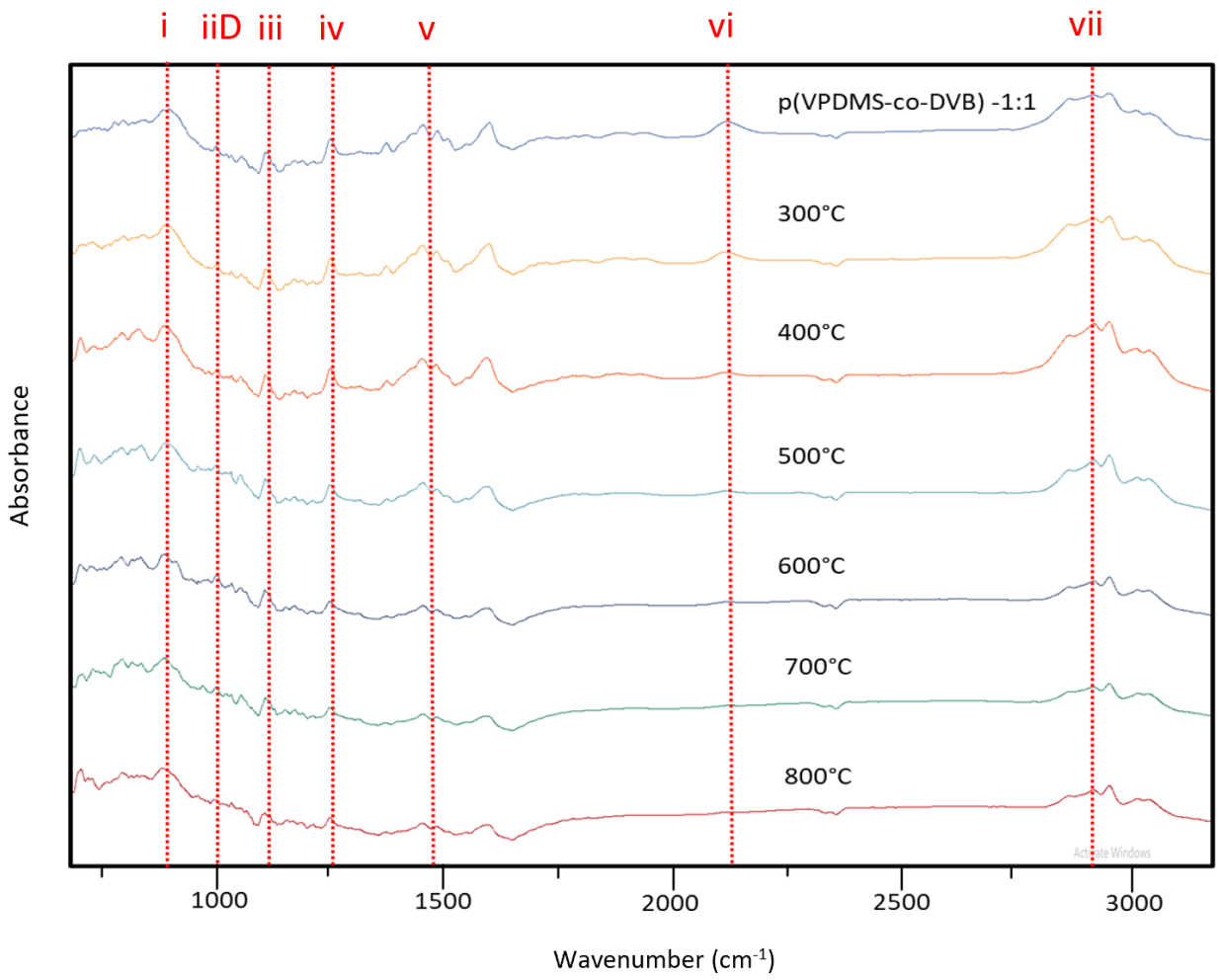

Figure 7: DRIFTS data for the 2:1 p(VPDMS-coDVB)-coated BaF_2. The dashed lines represent: (i) Si-C stretching, (iiD) Si-$(CH_2)_n$-Si stretching, (iii) Si-C_5H_6 stretching, (iv) symmetric Si-CH_3 stretching, (v) pDVB C-H and C=C stretching bands, (vi) Si-H stretching, and (vii) C-H hydrocarbon bonds from polyethylene bond and aromatic rings.

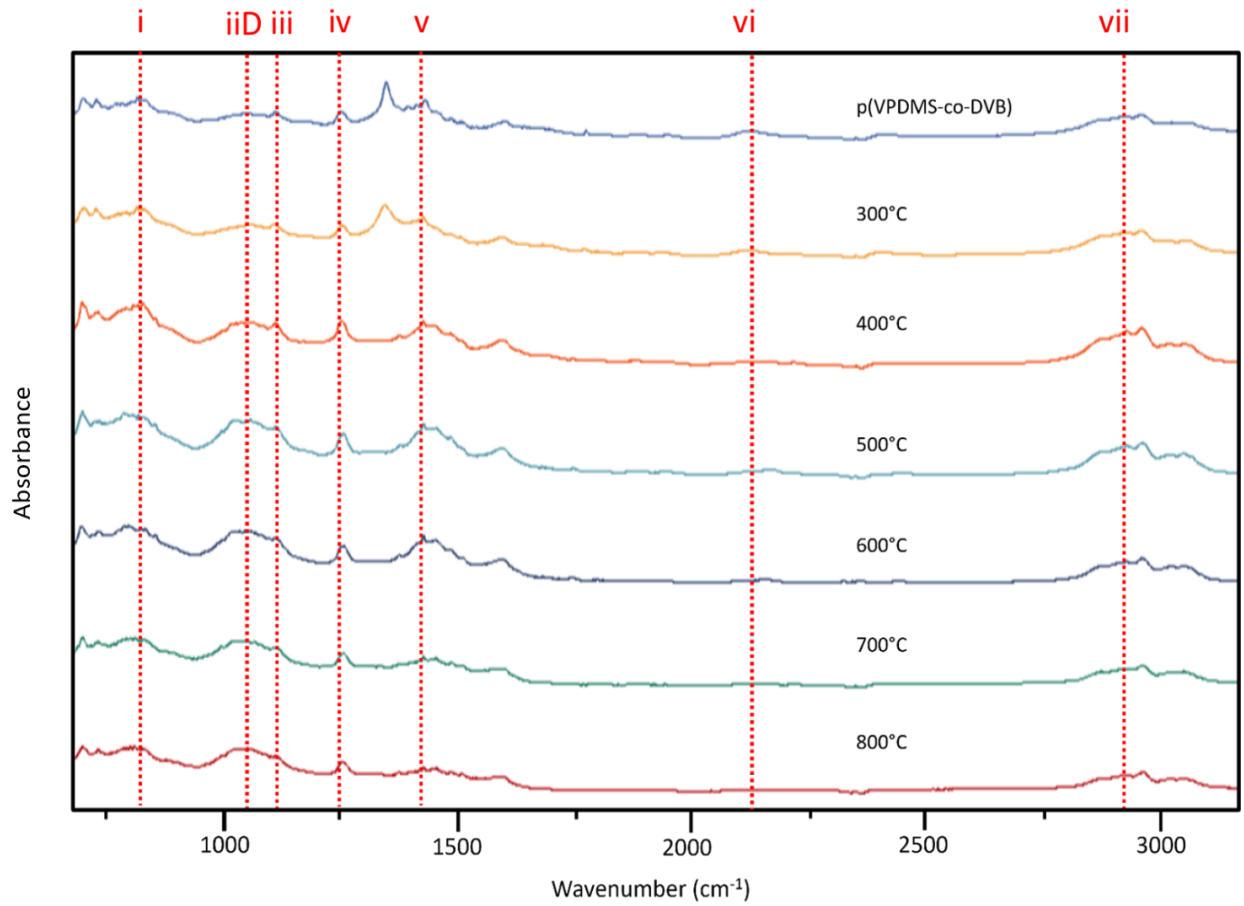

Figure 8: DRIFTS data for the 1:2 p(VPDMS-coDVB)-coated BaF_2. The dashed lines represent: (i) Si-C stretching, (iiD) Si-$(CH_2)_n$-Si stretching, (iii) Si-C_5H_6 stretching, (iv) symmetric Si-CH_3 stretching, (v) pDVB C-H and C=C stretching bands, (vi) Si-H stretching, and (vii) C-H hydrocarbon bonds from polyethylene bond and aromatic rings.

To better visualize the changes that the polymer goes through as it is being pyrolyzed, we baselined the IR spectra and performed an area-under-the-curve analysis to study the rates of disappearance of various functional groups. This analysis assumes the applicability of Lambert's Law[44], meaning that the concentration of the functional groups in the material is proportional to the absorbance of their corresponding individual peaks. This law has been shown previously[45,46] to be valid for a variety of organosilicon polymer materials, and we have no reason to believe that it does not apply to the organosilicon-type of materials studied here as well. The spectra area peaks were analyzed using Spectragryph and Origin Peak Fitting. The area between 2800 and 3100 cm^{-1} required peak fitting, as the peaks between 2800 and 3000 cm^{-1} are indicative of the C-H stretching for the sp^3 carbons in the polymer backbone, while the peaks between 3000-3100 cm^{-1}

are indicative of the sp^2 carbon C-H stretching of the aromatic rings from the DVB and Si-C_6H_5. The points collected during the "soak" periods, each spaced 100 °C apart, were averaged out to a single point.

Figure 9 shows the peak area for each functional group derived from the DRIFTS spectra. In the spectra, significant decreases in the areas of the functional groups did not occur until a pyrolysis temperature of approximately 200 °C. At ~280 °C (for the pVPDMS) and ~320 °C (for the 2:1 VPDMS:DVB copolymer), we begin to see a large decrease in the area of band v (aromatic C-H and C=C stretching bands), signifying, likely, the decomposition of the benzene rings. For the 1:1 and 1:2 VPDMS:DVB copolymers, the decrease of the band occurs at a higher a pyrolysis temperature, ~400 °C. We attribute this to the cross-linking ability of the DVB that helps keep the polymer intact at higher pyrolysis temperatures by slowing down the decomposition of the aromatic rings.

In the pVPDMS, 2:1 VPDMS:DVB, and 1:2 VPDMS:DVB copolymer spectra, the reduction of the aromatic rings area is subsequently followed by an increase in the area of the methyl (band iv) and polyethylene chain peaks (band iiD) in all of the copolymer spectra, which is indicative of possibly rearrangement to form hydrocarbon bridges between the Si atoms as well as loose hydrocarbon functional groups. The 1:1 VPDMS:DVB copolymer, in comparison, had a small amount of phenyl loss before 400 °C, but by a pyrolysis temperature of 420 °C, the peak areas for the phenyl, methyl, and ethylene groups had all started diminishing. By a pyrolysis temperature of 500 °C, both the methyl and ethylene areas in all of the polymers had started decreasing, with the 1:2 VPDMS:DVB copolymer having the highest pyrolysis temperature before these groups started decreasing. After this pyrolysis temperature, there is a sharp decrease in both the ethylene and methyl groups for all of the polymer films. Previously[8], we have seen that this is the temperature at which organic functional groups had started to cleave from organosilicon polymers. It is important to note that the decrease of the methyl and ethylene peak areas is delayed in the 1:2 VPDMS:DVB polymer, likely due to the high level of cross-linking compared to the other polymer films.

Past a temperature of 500 ºC, the peak areas of all functional groups continue to decrease, but the Si-C stretching bands stays relatively high. This is indicative of the polymer changing from a largely organosilicon structure into an Si-C type of network structure. At the pyrolysis temperature of 800 °C, only about 20% or less of the phenyl groups (band v) have remained in the

structure. The ethylene band remains very prominent in the spectra, of all polymers ranging between 40 to 60% of the original area. Among all polymers, the 1:2 VPDMS:DVB copolymer retained the most functionality, with approximately 60% of the methyl and ethylene groups remaining. This can be attributed to the larger amount of Si-$(CH)_n$-Si remaining in the structure, as indicated by the DRIFTS results.

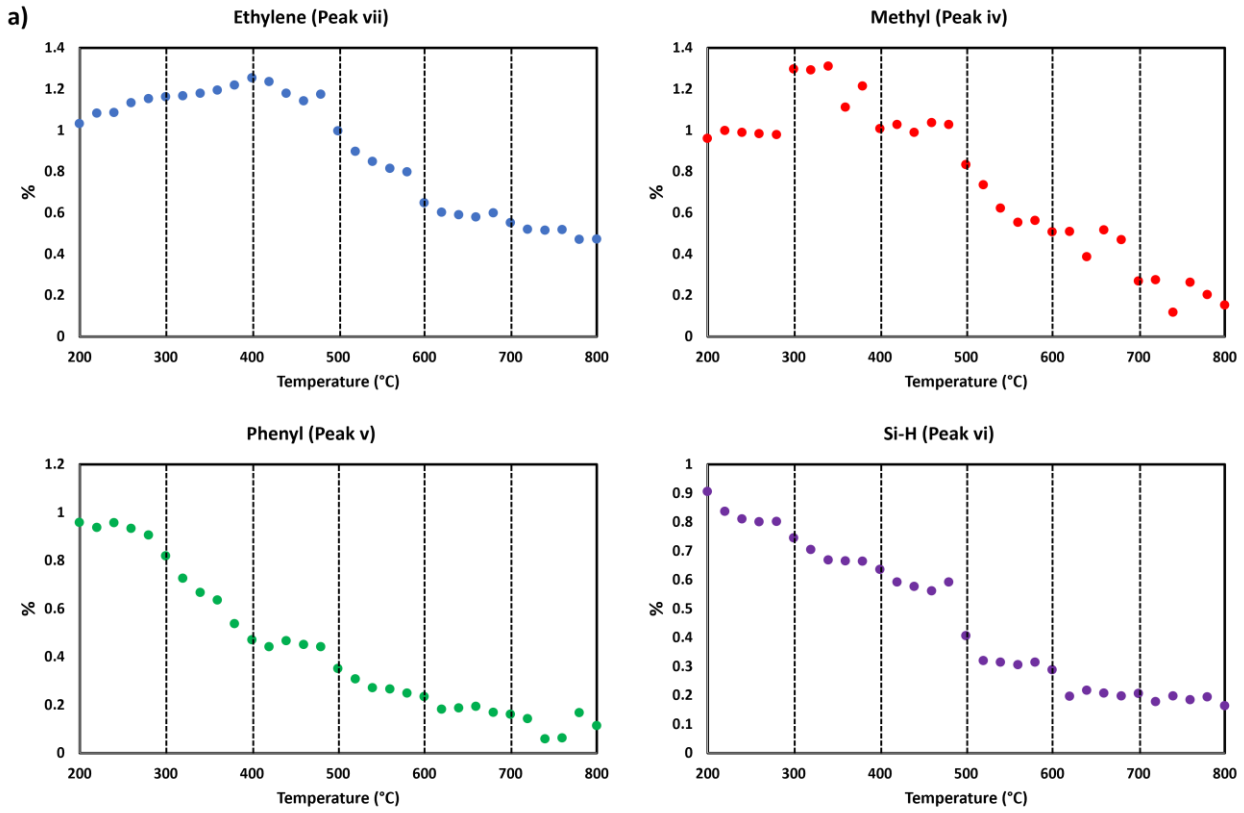

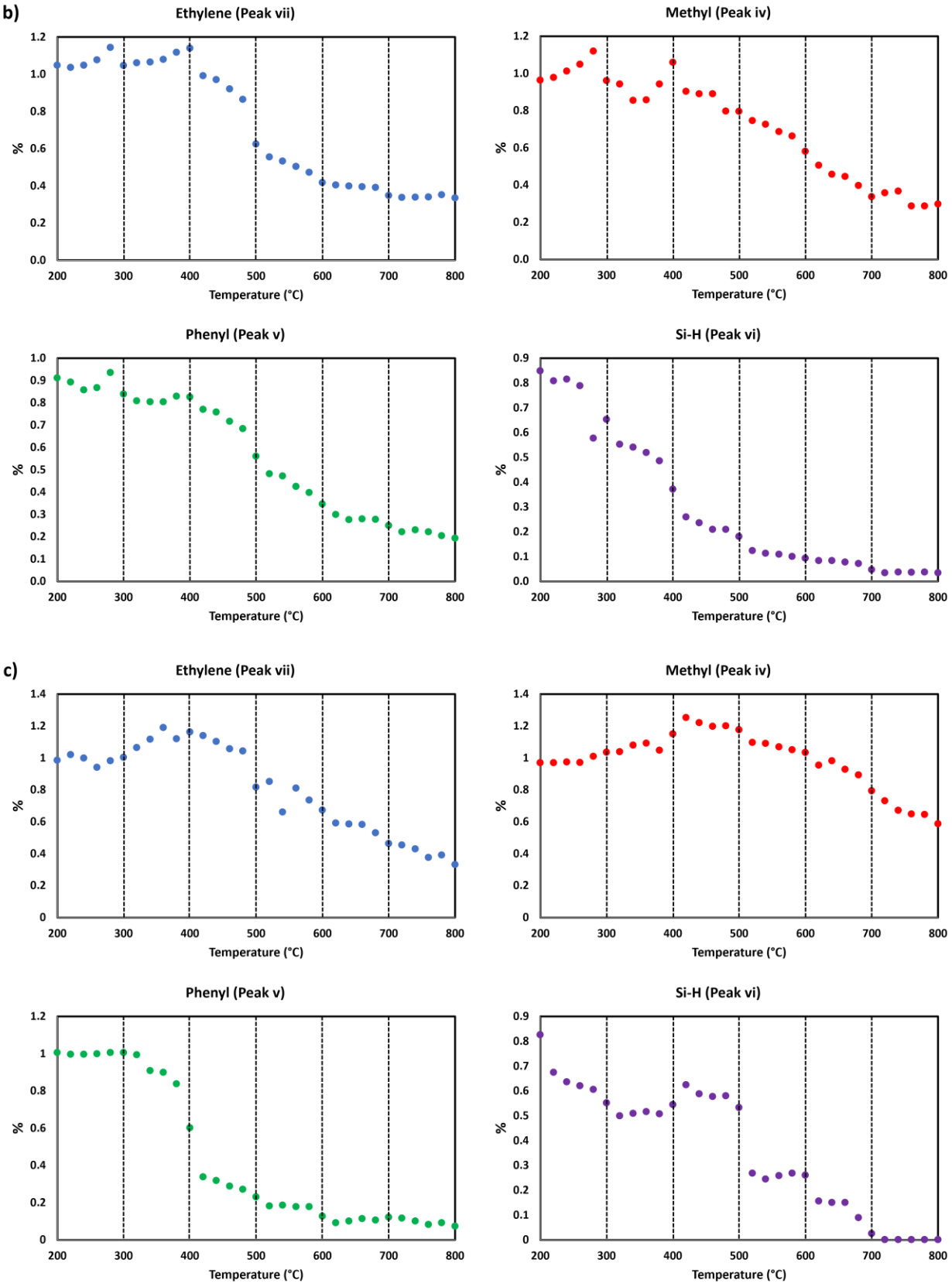
b)
Ethylene (Peak vii)
Methyl (Peak iv)
Phenyl (Peak v)
Si-H (Peak vi)
c)
Ethylene (Peak vii)
Methyl (Peak iv)
Phenyl (Peak v)
Si-H (Peak vi)
%
Temperature (°C)

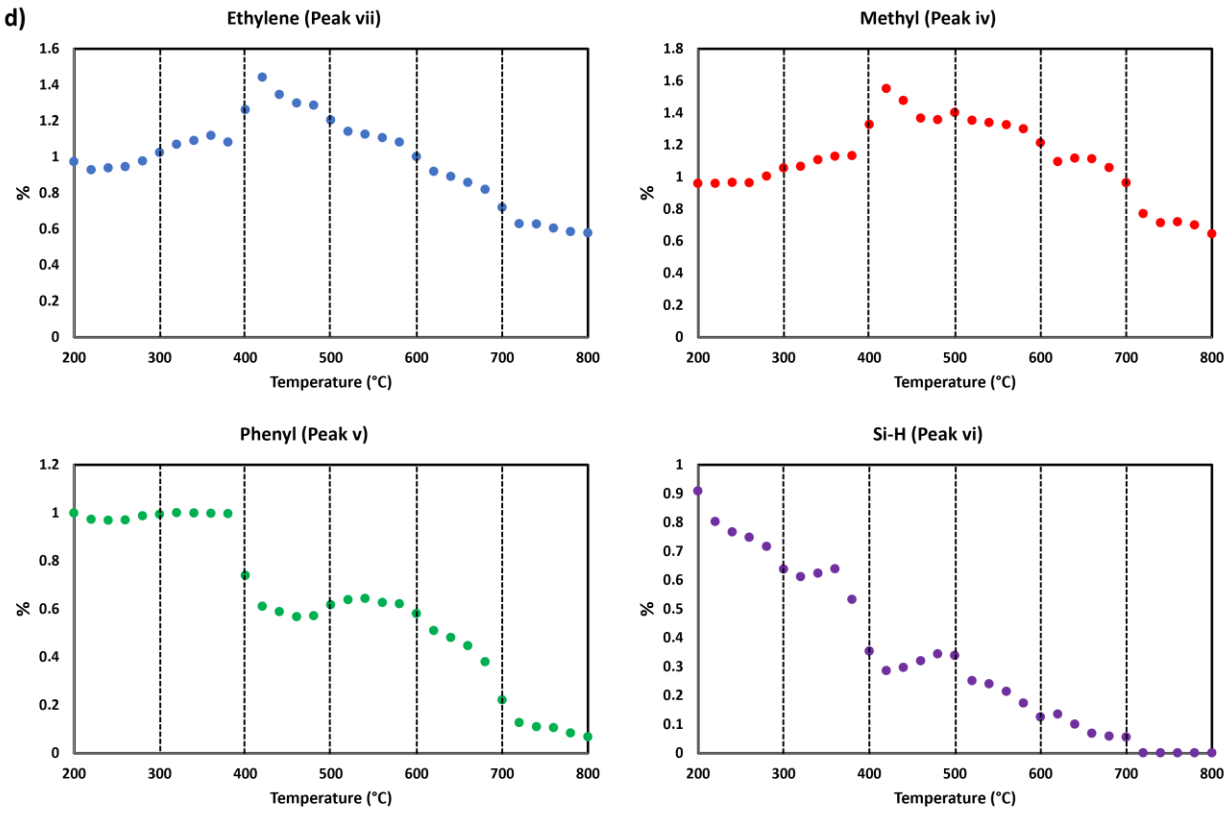

Figure 9: Functional group peak area change as a function of pyrolysis temperature for different polymer films: a) pVPDMS b) 1:1 p(VPDMS-co-DVB) c) 2:1 p(VPDMS-co-DVB) and d) 1:2 p(VPDMS-co-DVB).

Finally, to confirm the eventual transition of the polymers into a ceramic material, the polymer-coated powders were pyrolyzed ex-situ at a temperature of 1000 °C for 2 hr. in a graphite furnace. For these experiments, after placing the polymer samples inside, the furnace was first evacuated using a mechanical vacuum pump to remove any potential contaminants, and then flowing Ar was injected into the furnace to ensure that pyrolysis takes place under inert conditions. Post-pyrolysis, the powders were placed again in the DRIFTS chamber to carry out the analysis, with uncoated BaF_2 used as the background. The FTIR results of the polymer-coated powders pyrolyzed at the higher temperature obtained in the DRIFTS cell are shown in Figure 10. The spectra for the pVPDMS and the 1:1, 2:1, VPDMS:DVB copolymers only show a strong absorption band between 700 and 900 cm^{-1}, which is the primary anti-symmetric Si-C absorption band, as also reported by other groups [20,47] studying SiC with the DRIFTS technique. Specifically, the spectra contain no bands around 3000 cm^{-1}, which indicates that the long-chain carbon and aromatic bonds have been removed by this temperature. The 1:2 spectra also showed primarily a

rich SiC environment, but also contained a small absorption band around 1100 cm^{-1}, which is indicative of the presence of a network of Si-$(CH_2)_n$-Si bridges[26].

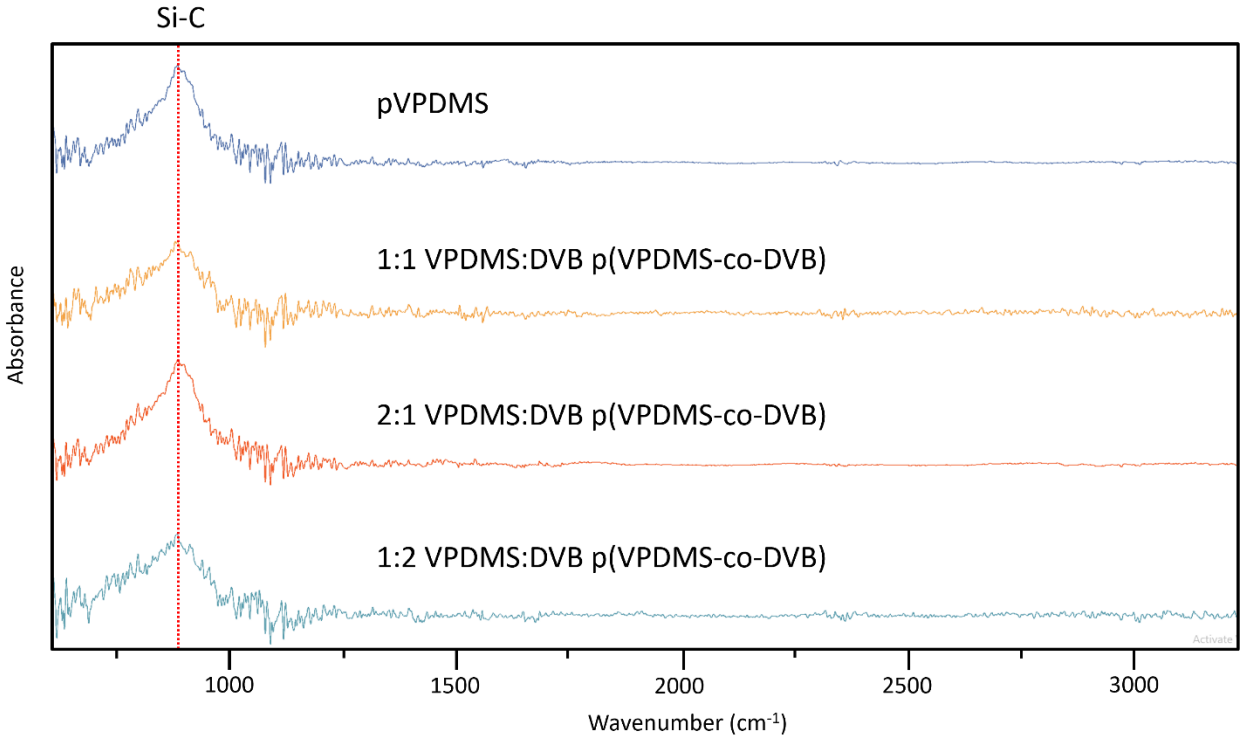

Figure 10. DRIFTS IR spectra of polymer-coated BaF_2 powders pyrolyzed at 1000 °C.

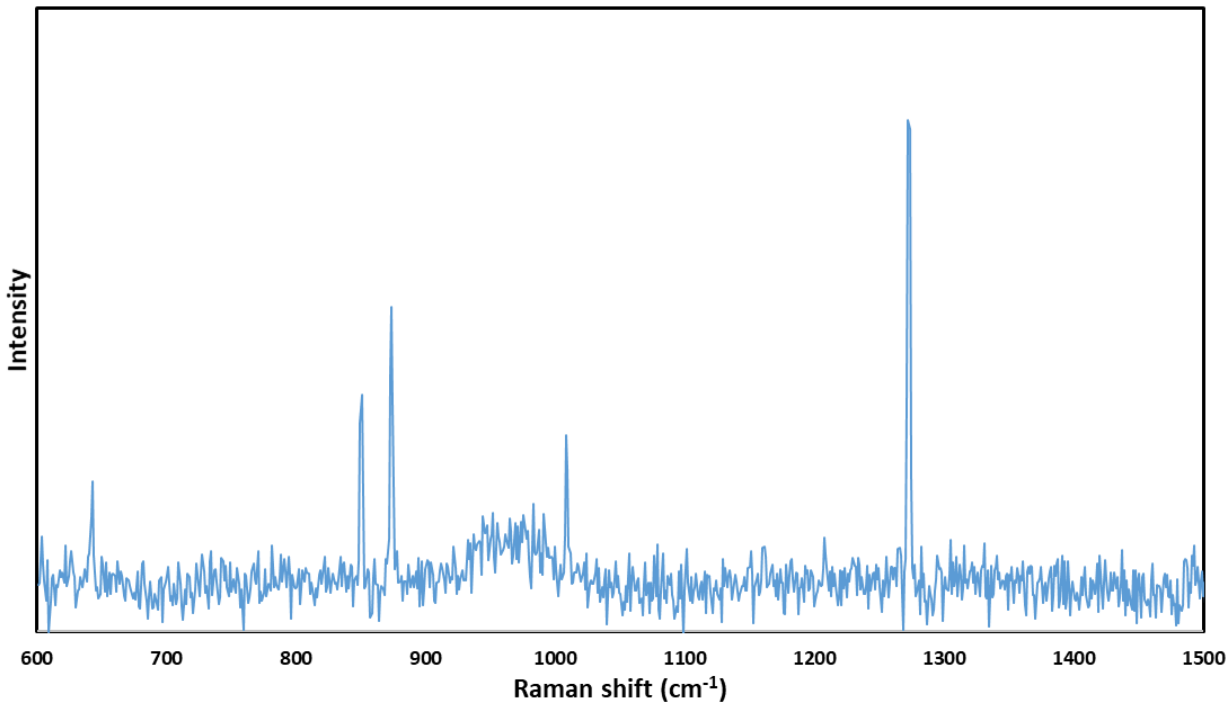

Figure 11. Raman spectrum for pyrolyzed 1:1 VPDMS:DVB co-polymer.

Table 3. Atomic Composition of the Pyrolyzed Polymer Films from EDS Analysis

Sample	Atomic Composition (%)				C/Si Ratio	Si/O Ratio
	Carbon	Silicon	Oxygen	Other		
pVPDMS	72.7	19.2	8.1	0	3.8	2.4
1:1 VPDMS:DVB	72.7	19.3	8.0	0	3.8	2.4
2:1 VPDMS:DVB	70.6	20.6	8.8	0	3.4	2.3
1:2 VPDMS:DVB	75.5	18.5	6.0	0	4.1	3.1

In order to determine the change in atomic composition of the polymer films, the polymer-coated wafers were placed in a tube furnace and pyrolyzed under flowing Ar at 1200 °C. Table 3 shows the atomic composition of the pyrolyzed films derived from the EDS analysis. As expected, there was a significant decrease in the carbon content of these films when compared to that (see Table 2) of the starting polymer films. The differences become more obvious when one compares the (C/Si) atomic ratio of the original films to the corresponding ratio of the pyrolyzed ones. The significant decrease in the (C/Si) ratio agrees with the DRIFTS results, which suggest a large

portion of the methyl and ethylene functional groups are evolved from the film as the pyrolysis temperature is increased. The (Si/O) atomic ratio differences between the original polymer films and their pyrolyzed counterparts are, on the other hand, significantly smaller as can be seen from comparing the two Tables, with the ratio remaining almost invariant for the 1:1 p(VPDMS-co-DVB) and 2:1 p(VPDMS-co-DVB copolymers. The EDS results suggest that the final ceramic is a silicon oxycarbide (SiO_xC_y) material, though it is likely that a fraction of its carbon content is free-standing carbon.

To further confirm these results, the Raman spectra of the pyrolyzed films on the Si wafers were taken, and the spectrum of the films (1:1 VPDMS:DVB) is shown in Figure 11. The results (Figure 11) show several distinct peaks that can be attributed to the Si-C environment. The region between 700 and 1000 cm^{-1} is, generally, attributed to Si-C bonding. [48] Two sharp peaks at approximately 850 cm^{-1} are attributed to the transverse optical phonon (TO) mode of Si-C. [49] There is also a broad peak centered at approximately 960 cm^{-1} that is attributed to amorphous Si-C.[49] There is also a sharp peak at approximately 1260 cm^{-1} that is attributed to the C-C bonding in the ceramic phase.[48] Additional XRD tests revealed no crystalline phase being present in the resulting films.

Thermogravimetric Analysis of Polymer Pyrolysis

Thermogravimetric Analysis (TGA) measurements can be used to determine the mass loss of materials and their stability during heating as a function of temperatures, and it is useful in determining the kinetics of polymer decomposition. For the TGA experiments in this study, the polymers were coated on BaF_2 powder and then pyrolyzed under flowing Ar. The heating program consisted of the following steps: First heating at a rapid rate of 5 °C/min to a temperature of 100 °C and "soaking" there for 2 hr, followed then by rapid heating to reach 300 °C, with a "soak" period there of 1 hr; this was then followed by several steps each consisting of a slow 100 °C temperature rise followed by an 1 hr "soak" period until a final pyrolysis temperature of 900 °C was reached, after which the sample was cooled down to room temperature.

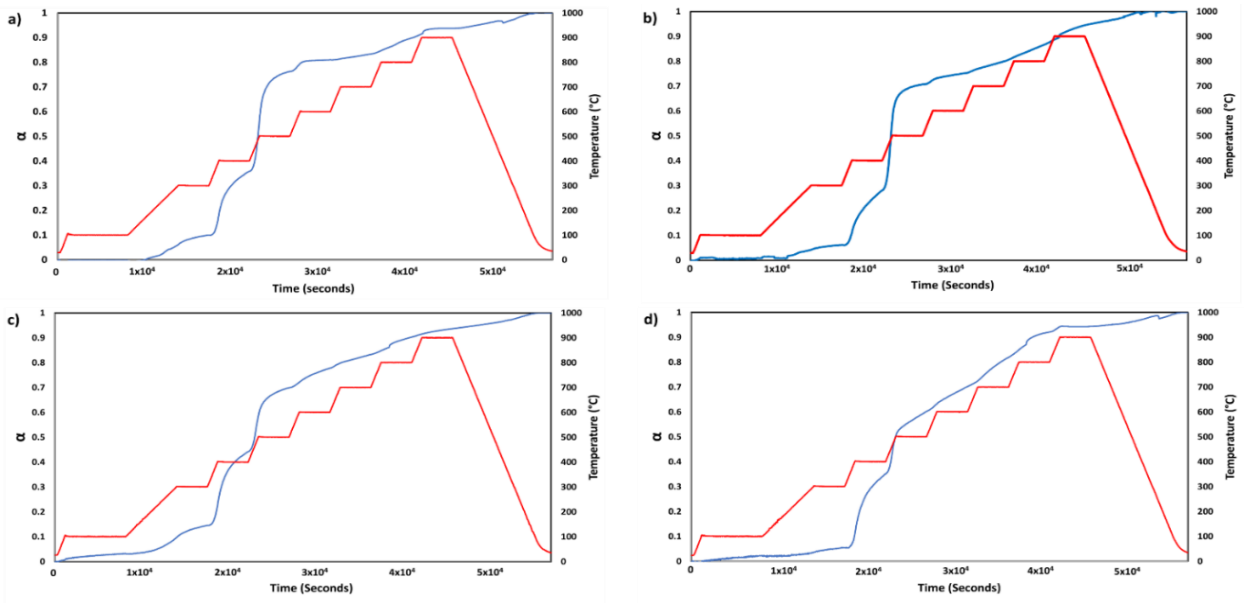

Figure 12: TGA graph showing the fraction of decomposition of the polymer films deposited on BaF_2: a) pVPDMS b) 1:1 VPDMS:DVB p(VPDMS-co-DVB) c) 2:1 VPDMS:DVB p(VPDMS-co-DVB) and d) 1:2 VPDMS:DVB p(VPDMS-co-DVB).

From the mass loss of the polymer during the TGA experiments, one can calculate the polymer decomposition fraction, α, at each time and corresponding temperature from the equation below, where m_i, m_t, and m_f are the initial mass, the mass at time t, and the final mass of the sample, respectively.

$$\alpha = \frac{m_i - m_t}{m_i - m_f} \qquad (1)$$

The results of the experiments are shown in Figure 12, which shows the decomposition fraction as a function of time. There was minimal mass loss before a pyrolysis temperature of 300 °C, with the 2:1 VPDMS:DVB copolymer experiencing the highest degree of decomposition at ~10%. This is in agreement with the DRIFTS experiments, where we observed minor losses in Si-H and phenyl groups, and the small change in mass can, potentially, be attributed to those losses. There were no major changes during the "soaking" period at 300 °C, but the loss in mass accelerated quickly after the temperature was raised beyond 300 °C. This is consistent with the scission of the aromatic rings from both the DVB and VPDMS components of the polymers, as observed from the DRIFTS results. The biggest change in α occurred between 400 °C and 600 °C. This large mass loss correlates well with the degradation of the aromatic groups, and the cleavage

of the polyethylene backbone and the methyl groups, as seen in the DRIFTS results. At a pyrolysis temperature of 500 °C, all four polymers had an α of ~0.5.

In the temperature range between 500 °C and 700 °C, the pVPDMS polymer had the highest increase in α, while the 1:2 VPDMS:DVB polymer had the slowest. At these pyrolysis temperatures, the DRIFTS results showed a significant decrease in the aromatic, methyl, and ethylene groups in the pVPDMS polymer. In comparison, the 1:2 VPDMS:DVB polymer initially had a significant loss of aromatic groups, followed by a low loss period between 500 °C and 600 °C, and finally an accelerated aromatic group loss after 600 °C. This indicates that the aromatic groups stayed intact in the 1:2 VPDMS:DVB polymer at higher pyrolysis temperatures than for all the other polymers, likely due to a higher degree of cross-linking. By a pyrolysis temperature of 900 °C, α for all films is above 0.9 and it also increases slowly during the "soaking" period. This observation is again consistent with the DRIFTS data that indicate that changes continue to happen in this temperature range albeit at a slower pace. These results show that the polymer pyrolysis process occurs in three distinct stages: Small changes for pyrolysis temperatures below ~350 °C, the main scission reactions taking place between 350 and 600 °C, with the final reactions occurring after 600 °C.

To more clearly visualize the changes that take place during pyrolysis, we plot in Figure 13 the derivative of weight, m_t, change with respect to time as a function of time. For all four polymers, there are two primary peaks observed in the derivative of weight change graph: A peak taking place at ~18,000 sec, just after the beginning of the "soak" period at 400 ºC, and another at 22,500 sec after the beginning of the "soak" period at 500 °C. Based on the DRIFTS data, the first peak corresponds to the scission of the aromatic rings from the polymer network structure, while the second peak corresponds to the loss of the methyl and ethylene groups after the aforementioned Kumada rearrangement of the silicon-carbon bridges. So, the derivative of weight change allows us to confirm that the primary scission reactions for all of the polymers occur between 400 °C and 600 °C. There are smaller size peaks at later times during the pyrolysis process, which correspond to more subtle changes in the material's structure as it continues to evolve into a Si-C type of material.

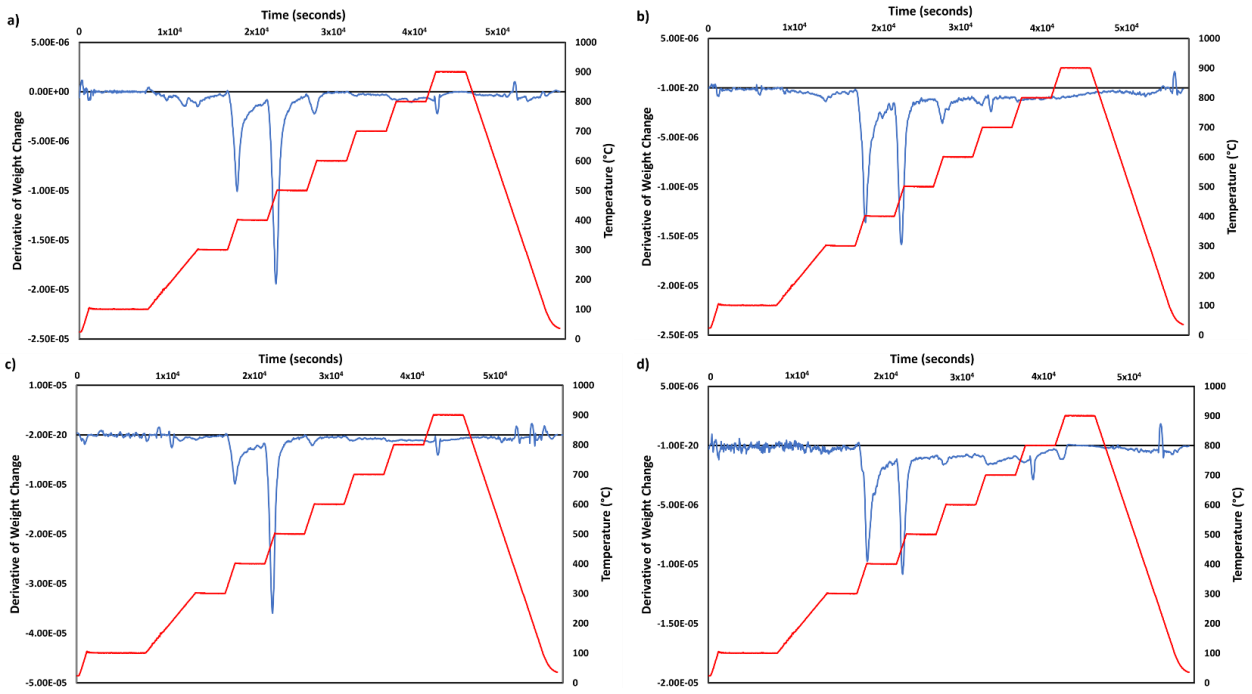

Figure 13: Weight change loss during polymer pyrolysis under TGA experiments for polymer films a) pVPDMS b) 1:1 VPDMS:DVB p(VPDMS-co-DVB) c) 2:1 VPDMS:DVB p(VPDMS-co-DVB) and d) 1:2 VPDMS:DVB p(VPDMS-co-DVB)

Inorganic Residue Yield

To determine the inorganic residue yield of the samples, the polymers were deposited on porous SiC tablets and subsequently pyrolyzed. The fabrication technique for these tablets can be found elsewhere.[7] The mass of these tablets was measured before polymer deposition, after deposition, and after pyrolysis. The equation for calculating the ceramic yield is shown below, and the measured ceramic yields for the four polymers are shown in Table 4.

$$Inorganic\ residue\ yield = \frac{Weight\ of\ Ceramic\ Generated}{Polymer\ Deposited} = \frac{Post{-}Pyrolysis\ Weight{-}Pre{-}Deposition\ Weight}{Post{-}Deposition\ Weight{-}Pre{-}Deposition\ Weight} \quad (2)$$

It can be seen from Table 4, that the inorganic residue yield for pVPDMS was the lowest among the four polymers studied, less than 10%. Likewise, it can be seen that the 1:1 and 1:2 VPDMS:DVB copolymers had relatively low yield as well, with yields of approximately 13%. The polymer with the highest yield post-pyrolysis was the 2:1 VPDMS:DVB copolymer, with a

yield of above 21%. This then gives credence to the hypothesis that cross-linking the polymer prior to its pyrolysis does, indeed, help with retention of the polymer mass during pyrolysis and the generation of a greater quantity of the inorganic film (compare the pVPDMS inorganic residue yield with that of 2:1 VPDMS:DVB copolymer). There is, however, an optimal DVB content in the original polymer, with too high of a DVB to VPDMS ratio resulting in a lower inorganic residue yield. This can be attributed to the pDVB polymer chains disintegrating during the earlier stages of pyrolysis.

Table 4. Inorganic residue yield of various polymer films post-pyrolysis

Sample	**Ceramic Yield (%)**
pVPDMS	9.09
2:1 VPDMS:DVB	21.74
1:1 VPDMS:DVB	12.50
1:2 VPDMS:DVB	13.04

Film Thickness Change

Profilometry was used to analyze the changes in the thicknesses of the thin films as a function of pyrolysis temperature. Copolymer films with thicknesses of 10 μm, as measured by the interferometer, were deposited on Si wafers with electric tape placed on one side of the wafer in order to create an edge for the profilometry measurements. Before pyrolysis, the polymer film thicknesses were measured by a stylus profilometer using the edge of the polymer film. The films were then heated in a tube furnace under flowing Ar to set temperatures at a heating rate of 2 °C/min, and they had a "soak" period of 2 hr at the desired set temperature. After the "soaking" period, the wafers were cooled to room temperature at a cooling rate of 3 °C/min before they were removed from the tube furnace. The film thickness of the pyrolyzed samples was then measured using profilometry. The equation for calculating the thickness change is shown below, and the thickness change for each polymer film as a function of temperature is shown in Figure 14.

$$Thickness\ change = \frac{Thickness\ of\ polymer\ post-deposition}{Thickness\ of\ polymer\ pre-deposition} x\ 100 \qquad (3)$$

There were no significant changes in the polymer film thickness when heated from room temperature to 200 °C. However, by a pyrolysis temperature of 300 °C, the thicknesses of the pVPDMS and 2:1 VPDMS:DVB copolymer films had decreased significantly, with thicknesses being equal to ~71% and ~83% of the original bulk polymer thickness, respectively. In comparison, the 1:1 and 1:2 VPDMS:DVB copolymer films showed significantly less change in thicknesses, with both retaining over 90% of their original thickness. This can be attributed to the fact that higher incorporation of DVB overall leads to higher cross-linking, which helps with polymer mass retention at lower pyrolysis temperatures until the scissioning of the DVB moieties from the polymer commences. The most significant change in the thickness of all pyrolyzed films occurred between pyrolysis temperatures of 300 °C and 400 °C. All film thicknesses dropped to less than 40% of their initial bulk polymer film thicknesses, with the largest being the thickness of the 1:2 VPDMS:DVB copolymer at ~35% of its original value and the smallest being the one of the 2:1 VPDMS:DVB copolymer film at ~21%. After a pyrolysis temperature of 400 °C, all of the films showed continued loss in thickness until a pyrolysis temperature of 900 °C, with the pVPDMS film showing the highest thickness retention between 500 °C and 900 °C, and the 2:1 VPDMS:DVB copolymer showing the least thickness retention in the same range. By a pyrolysis temperature of 900 °C, the thickness of all the polymer films had reduced to between 8 and 10 % of the original bulk polymer thickness, with the pVPDMS showing the highest retention at 11.75% and the 1:1 and 2:1 VPDMS:DVB copolymers showing the least retention at ~9% of their original bulk film thickness.

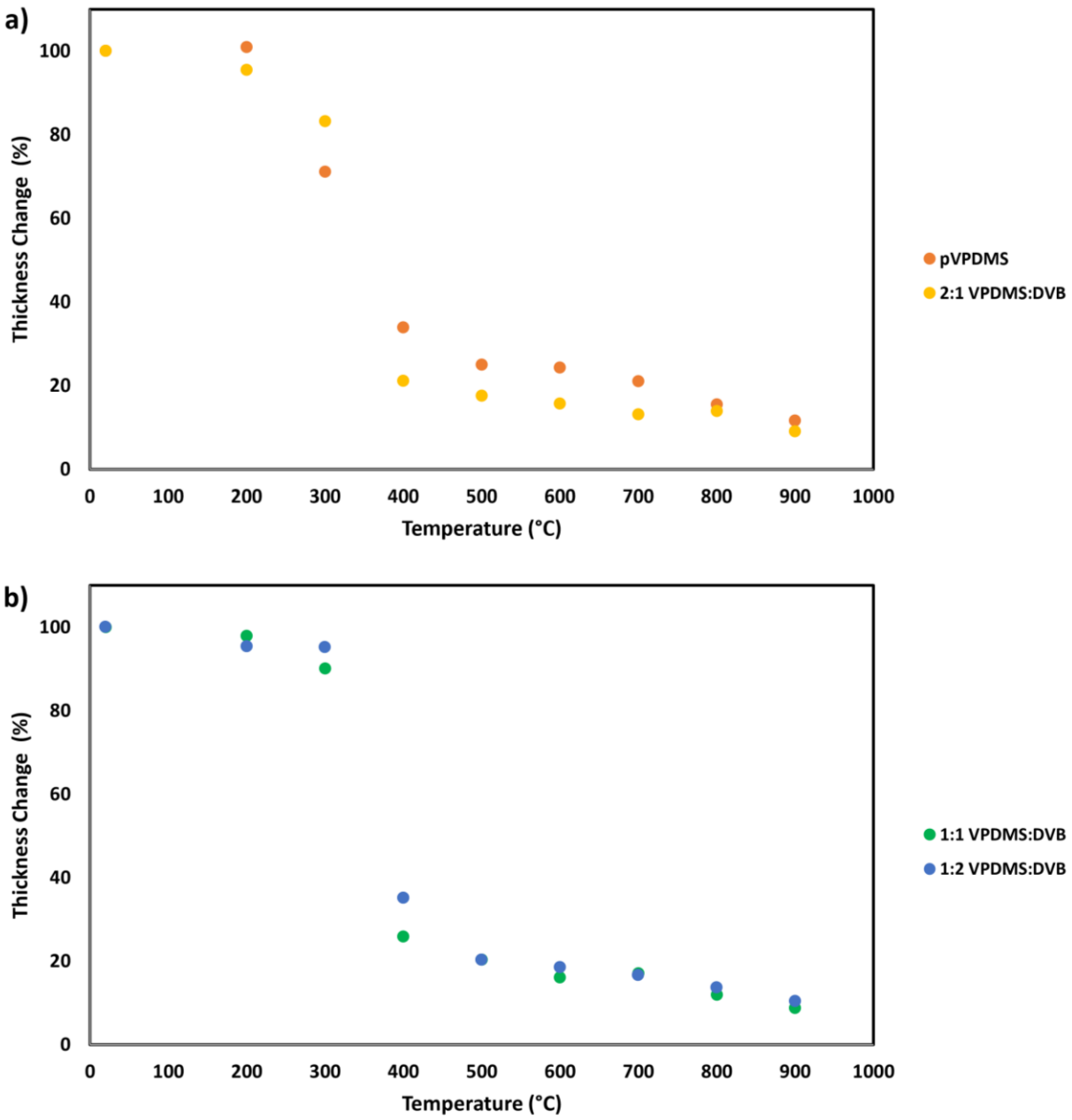

Figure 14: Thickness change of the various polymer films as a function of temperature for a) the pVPDMS and the 2:1 VPDMS:DVB copolymer; b) the 1:1 VPDMS:DVB and the 1:2 VPDMS:DVB copolymers.

Conclusion

In this project, we studied the deposition of pre-ceramic polymers on inorganic powder substrates and their subsequent pyrolysis to form ceramic films. Specifically, we systematically studied the deposition of the copolymer (p(VPDMS-co-DVB)) via PECVD at various reactor

monomer feed compositions on two different powder substrates (KBr and BaF_2) and their subsequent pyrolysis for temperatures up to 1000 ºC.

We have selected in our studies a monomer (VPDMS) and a crosslinking agent (DVB) for preparing the pre-ceramic polymer materials with no oxygen in their structure, which makes them appropriate to use to fabricate Si-C type films upon pyrolysis. However, some minor quantity of oxygen gets incorporated into the structure of the polymer film either during the preparation stage or, most likely, during the sample transfer from the PECVD chamber into the pyrolysis furnace (current efforts in the group focus on the design and construction of a PECVD system that encompasses in situ pyrolysis, thus avoiding sample exposure to atmospheric conditions). Analysis of the structural changes of the polymer as it undergoes pyrolysis indicates that at least some of that initial oxygen is retained in the structure to eventually form a SiO_xCy ceramic.

The DRIFTS technique was used to study in situ the mechanism, to track the fate of the various polymer functional groups, and to identify the various structural rearrangements that take place during the pyrolysis process. The TGA method was used to study the mass loss of the film during pyrolysis. Combining the TGA and DRIFTS analysis results helped to shed additional light into the mechanism by which the original polymer precursor converts into the final ceramic via pyrolysis. We also performed ex-situ profilometry and ceramic yield measurements of the films in order to determine the change in film properties post-pyrolysis. We found that the film thicknesses decreased by up to 90% at 900 °C, confirming the results of the DRIFTS and TGA experiments.

Acknowledgements

The authors acknowledge the support of the National Science Foundation (Award# CMMI-2012196). EDS data were acquired at the Core Center of Excellence in Nano Imaging at the University of Southern California.

References:

[1] Ivashchenko, L., Vasin, A., Ivashchenko, V., Ushakov, M., and Rusavsky, A. Blue Light Emission from PECVD Deposited Nanostructured SiC, Mater. Res. Soc. Symp. Proc., 2006, 910

[2] Carlsson, D. J.; Cooney, J. D.; Gauthier, S.; Worsfold, D. J. Pyrolysis of Silicon-Backbone Polymers to Silicon Carbide, Am. Ceram. Soc. 1990, 73 (2), 237–241.

[3] Yakimova, R., Petoral, R., Yazdi, G., Vahlberg, C., Spetz, A., and Uvdal, K. Surface Functionalization and Biomedical Applications Based on SiC, J. Phys. D: Appl. Phy., 2007, 40, 6435.
[4] Bourenane, K., Keffous, A., Nezzal, G., Bourenane, A., Boukennous, Y., and Boukezzata, A. Influence of Thickness and Porous Structure of SiC Layers on the Electrical Properties of Pt/SiC-pSi and Pd/SiC-pSi Schottky Diodes for Gas Sensing Purposes. Sens. Actuators B: Chem., 2008, 129, 2, 612-620.
[5] Kolar, F., Machovic, V., Svitilova, J., and Borecka, L. Structural Characterization and Thermal Oxidation Resistance of Silicon Oxycarbides Produced by Polysiloxane Pyrolysis, Mater. Chem. Phys., 2004, 86, 1, 88-98
[6] Eray, E., Boffa, V., Jorgensen, M., Magnacca, G., and Candelario, V. Enhanced Fabrication of Silicon Carbide Membranes for Wastewater Treatment: From Laboratory to Industrial Scale, J. Membrane Science, 2020, 606, 118080
[7] Elyassi, B., Sahimi, M., and Tsotsis, T. Silicon Carbide Membranes for Gas Separation Applications, J. Membrane Science, 2007, 288, 1-2, 290-297.
[8] Dabir, S., Deng, W., Sahimi, S., and Tsotsis, T. Fabrication of Silicon Carbide Membranes on Highly Permeable Supports, J. Membrane Science. 2017, 537, 1, 239-247.
[9] Mourhatch, R., Tsotsis, T., and Sahimi, M. Network Model for the Evolution of the Pore Structure of Silicon-Carbide Membranes During Their Fabrication, J. Membrane Science. 2010, 356, 1, 138-146.
[10] Liu, D., Hu, P., Chen, G., and Han, W. Fabrication of Silicon Carbide Coating on Mullite Fiber-reinforced Mullite Matrix Composite via Dip-Coating, Ceram. Int.. 2018, 44, 2, 2584-2586
[11] Nechanicky, M., Chew, K., Sellinger, A., and Laine, R. α-Silicon Carbide/β-Silicon Carbide Particulate Composites via Polymer Infiltration and Pyrolysis (PIP) Processing using Polymethylsilane, J. Eur. Ceram. Soc., 2000, 20, 4, 441-451
[12] Seidel, S.; Riche, C.; Gupta, M. Chemical Vapor Deposition of Polymer Films, Encycl. Polym. Sci. Technol. 2011.
[13] Henry, A., Hassan, J., Bergman, J., Hallin, C., and Janzen, E. Thick Silicon Carbide Homoepitaxial Layers Grown by CVD techniques., Chem. Vap. Deposition. 2006, 12, 475-482.
[14] Pedersen, H., Leone, S., Kordina, O., Henry, A., Nishizawa, S., Koshka, Y., and Janzen, E. Chloride-Based CVD Growth of Silicon Carbide for Electronics Applications, Chem. Rev., 2012, 112, 4, 2434-2453.
[15] Chen, E., Du, G., Zhang, Y., Qin, X., Lai, H., and Shi, W. RF-PECVD Deposition and Optical Properties of Hydrogenated Amorphous Silicon Carbide Thin Films, Ceram. Int., 2014, 40, 9791-9797
[16] Flannery, A., Mourlas, N., Storment, C., Tsai, S., Tan, S., Heck, J., Monk, D., Kim, T., Gogoi, B., and Kovacs, G. PECVD Silicon Carbide as a Chemically Resistant Material for Micromachined Transducers, Sens. Actuator A Phys., 1998, 70, 48-55
[17] Cogan, S., Edell, D., Guzelian, A., Liu, Y., and Edell, R. Plasma-enhanced Chemical Vapor Deposited Silicon Carbide as an Implantable Dielectric Coating, J. Biomed. Mater. Res., 2003, 67A, 3, 856-867
[18] Pages, X., Rouessac, V., Cot, D., Nabias, G., and Durand, J. Gas Permeation of PECVD Membranes Inside Alumina Substrate Tubes, Sep. Purif. Technol., 2001, 25, 399-406
[19] Huran, J. Valovic, A., Kobzec, A.P., Balalykin, N.I., Kucera, M., Hascik, S., Malinovsky, L., and Kovacova, E. Structural and Physical Characteristics of PECVD Nanocrystalline Silicon Carbide Thin Films, Physics Procedia, 2012, 32, 303-307
[20] Wei, J., Chen, B., Poenar, D., Lee, Y., and Iliescu, C. Low-stress PECVD Amorphous Silicon Carbide Layers for Biomedical Application, Proc. SPIE, Micro- and Nanotechnology: Materials, Processes, Packaging, and Systems IV, 2009, 72690C
[21] Eom, J., Kim, Y., and Raju, S. Processing and Properties of Macroporous Silicon Carbide Ceramics: A Review, J. Asian Ceram. Soc., 2013, 1, 220-242
[22] Nguyen, B., Dabir, S., Tsotsis, T., and Gupta, M., Fabrication of Hydrogen-Selective Silica Membranes via Pyrolysis of Vapor Deposited Polymer Films, Ind. Eng. Chem. Res., 2019, 58, 15190-15198.
[23] S. H. Baxamusa, S. G. Im, and K. K. Gleason, Phys. Chem. Chem. Phys. 11, 5227 (2009).
[24] Burns, G., Taylor, R., Xu, Y., Zangvil, A., and Zank, G. High-Temperature Chemistry of the Conversion of Siloxanes to Silicon Carbide, Chem. Mater. 1992, 4, 1313-1323
[25] L. Martinu, O. Zabeida, J.E. Klemberg-Sapieha, Plasma-enhanced Chemical Vapor Deposition of Functional Coatings, in: Handb. Depos. Technol. Film. Coatings, Elsevier, 2010, pp. 392–465
[26] Freitas, A., Maciel, C., Rodrigues, J., Ribeiro, R., Delgado-Silva, A., and Rangel, E. Organosilicon Films Deposited in Low-Pressure Plasma From Hexamethyldisiloxane – A Review, Vacuum, 2021, 194, 110556

[27] Daniel, A., Pen, C., Archambeau, C., and Reniers, F. use of a PECVD-PVD Process for the Deposition of Copper Containing Organosilicon Thin Films on Steel, Appl. Surf. Sci., 2009, S82-S85
[28] Bae. I, Cho, S., Lee, S., Kim, Y., and Boo, J. Growth of Plasma-Polymerized Thin Films by PECVD Method and Study on Their Surface and Optical Characteristics, Surf. Coat. Technol., 2005, 193, 142-146
[29] Cheng, C., and Gupta, M. Solvent-Free Synthesis of Selectively Wetting Multilayer and Janus Membranes, Adv. Mater. Interfaces, 2020, 7, 20, 2001103
[30] ThermoSpectraTech. *COLLECTOR ™ II User ' s Manual*.
[31] Raj, R.; Pederiva, L.; Narisawal, M.; Soraru, G. D. On the Onset of Fracture as a Silicon-Based Polymer Converts into the Ceramic Phase, J. Am. Ceram. Soc. 2018, *102* (3), 924–929.
[32] Zhao, J., Wang, M., and Gleason, K.K. Stabilizing the Wettability of Initiated Chemical Vapor Deposited (iCVD) Polydivinylbenzene Thin Films by Thermal Annealing, Adv. Mater. Interfaces, 2017, 4, 1700270
[33] Moni, P., Mohr, A., and Gleason, K. Growth Rate and Cross-Linking Kinetics of Poly(divinyl benzene) Thin Films Formed via Initiated Chemical Vapor Deposition, Langmuir, 2018, 34, 6687-6696
[34] Ermakova, E., Sysoev, S., Nikulina, L., Tsyrendorzhieva, I., Rakhlin, V., and Kosinova, M. Trimethyl(phenyl)silane – a Precursor for Gas Processes of SiCx:H Film Deposition: Synthesis and Characterization, Mod. Electron. Mater., 2015, 1, 114-119
[35] Kobayashi, S. IR Spectroscopic Study of Silicon Nitride Films Grown at a Low Substrate Temperature Using Very High Frequency Plasma-Enhanced Chemical Vapor Deposition, World J. Condens. Matter Phys., 2016, 6, 287-293
[36] Dos Santos, D., Vechiato-Filho, A., Pesqueria, A., Guiotti, A., Rangel, E., da Cruz, N., and Goiato, M. Effect of Nonthermal Plasma Treatment on the Surface of Dental Resins Immersed in Artificial Saliva, J. Polym. Eng., 2016, 36, 8, 785-793
[37] Rangel, R., Cruz, N., and Rangel, E. Role of the Plasma Activation Degree on Densification of Organosilicon Films, Materials, 2020, 13, 1, 25
[38] Ivashchenko, L., Vasin, A., Ivashchenko, V., Ushakov, M., and Rusavsky, A. Blue Light Emission from PECVD Deposited Nanostructured SiC, Mater. Res. Soc. Symp. Proc., 2006, 910
[39] Kolar, F., Machovic, V., Svitilova, J., and Borecka, L. Structural Characterization and Thermal Oxidation Resistance of Silicon Oxycarbides Produced by Polysiloxane Pyrolysis, Mater. Chem. Phys., 2004, 86, 1, 88-98
[40] Breuning, T. Study of Pyrolysis of Polysilazane Precursor in Si-C-(O,N) System, J. Anal. Appl. Pyrolysis., 1999, 49, 1-2, 43-51
[41] Moene, R., Makkee, M., and Mouljin, J.A. High Surface Area Silicon Carbide as Catalyst Support Characterization and Stability, Applied Catalysis A: General, 1998, 167, 321-330
[42] Straus, S., Madorsky, S. Thermal Stability of Polydivinylbenzene and of Copolymers of Styrene With Divinylbenzene and With Trivinylbenzene, J. Res. Natl. Bur. Stand A Phys. Chem., 1961, 243-248
[43] Schiavon, M.A., Radovanovic, E., Yoshida, I., Microstructural Characterization of Monolithic Ceramic Matrix Composites from Polysiloxane and SiC Powder, Powder Technology, 2001, 232-241
[44] Shi, Z., Sanguinito, S., Goodman, A., Jessen, K., and Tsotsis, T. Investigation of Mass Transfer and Sorption in CO2/Brine/Rock Systems via In Situ FT-IR, Ind. Eng. Chem. Res., 2020, 59, 20181-20189
[45] Rich, S., Mille, V., Vivien, C., Godey, S., and Supiot, P. Kinetics of RPECVD Organosilicon Polymer Post-treatment in a N_2/O_2 Microwave Plasma Remote Afterglow, Plasma Process Polym, 2010, 7, 9-10, 775-784
[46] Zhang, L., Ljazouli, R., Lefaucheux, P., Tillocher, T., Dussart, R., Mankelevich, Y., Marneffe, J., Gendt, S., and Baklanov, M. Damage Free Cryogenic Etching of a Porous Organosilica Ultralow-k Film, Electrochem. Solid-State Lett., 2013, 2, N5
[47] Tsuge, A., Uwamino, Y., and Ishizuka, T. Determination of Silicon Dioxide in Silicon Carbide by Diffuse Reflectance Infrared Fourier Transform Spectrometry, Appl. Spectrosc., 1986, 40, 3, 310-313
[48] Ward, Y., Young, R.J., and Shatwell, R.A. Application of Raman Microscopy to the Analysis of Silicon Carbide Monofilaments, J. Mater. Sci., 2004, 39, 6781-6790

For Table of Contents use only:

[49] Nakashima, S., Mitani, T., Tomobe, M., Kato, T., and Okumura, H. Raman Characterization of Damaged Layers of 4H-SiC Induced by Scratching, AIP Adv., 2016, 6, 015207

For Table of Contents use only: